Discovery of novel, drug-like ferroptosis inhibitors with in vivo efficacy

Discovery of Novel, Drug-like Ferroptosis Inhibitors with In Vivo Efficacy

*Lars Devisscher [#] [a], Samya Van Coillie [#] [b,c], Sam Hofmans [a], Dries Van Rompaey [a], Kenneth Goossens [a], Eline Meul [b,c], Louis Maes [d], Hans De Winter [a], Pieter Van Der Veken [a], Peter Vandenabeele [b,c,e], Tom Vanden Berghe [#] * [b,c], Koen Augustyns [#] * [a]*

[a] Laboratory of Medicinal Chemistry, University of Antwerp, Universiteitsplein 1, 2610 Antwerp, Belgium.

[b] Molecular Signalling and Cell Death unit, VIB Center for Inflammation Research, Technologiepark 927, 9052 Ghent, Belgium.

[c] Department of Biomedical Molecular Biology, Ghent University, 9000 Ghent, Belgium.

[d] Laboratory for Microbiology, Parasitology and Hygiene, University of Antwerp, Universiteitsplein 1, 2610 Antwerp, Belgium.

[e] Methusalem Program, Ghent University, Ghent, Belgium.

[#] These authors contributed equally.

Keywords: ferroptosis, regulated necrosis

ABSTRACT

Ferroptosis is an iron-catalysed, non-apoptotic form of regulated necrosis that results in oxidative lipid damage in cell membranes that can be inhibited by the radical-trapping antioxidant Ferrostatin-1 (Fer-1). Novel inhibitors derived from the Fer-1 scaffold inhibited ferroptosis potently but suffered from solubility issues. In this paper, we report the synthesis of a more stable and readily soluble series of Fer-1 analogues that potently inhibit ferroptosis. The most promising compounds (**37, 38** and **39**) showed an improved protection compared to Fer-1 against multi-organ injury in mice. No toxicity was observed in mice after daily injection of **39 (UAMC-3203)** for 4 weeks. **UAMC-3203** inserts rapidly in a phospholipid bilayer *in silico*, which aligns with the current understanding of the mechanism of action of these compounds. Concludingly, these analogues have superior properties compared to Fer-1, show *in vivo* efficacy and represent novel lead compounds with therapeutic potential in relevant ferroptosis-driven disease models.

INTRODUCTION

The classical view that a cell can undergo cell death by either one of two distinct prototypic cell death pathways, apoptosis or necroptosis, has become invalid.[1] While apoptosis is carried out following a strict mechanism involving cellular proteases called caspases, necroptosis critically depends on the concerted action of several enzymes such as the receptor interacting protein kinases (RIPK) and the mixed lineage kinase domain like pseudokinase (MLKL).[2–4] To date, several other forms of regulated necrosis each with their distinctive pathways and effector molecules are described.[5,6]

One molecule that is able to induce a form of regulated necrosis is erastin.[7] Erastin interacts with mitochondrial voltage-dependent anion channels (VDACs) which induces a RAS-RAF-MEK-dependent form of cell death due to the formation of reactive oxidative species (ROS).[8] Subsequently, the Stockwell lab found that erastin also inhibits the membrane-bound cystine/glutamate antiporter System X_c^-, which accounts for the induction of a non-apoptotic form of cell death.[9] This novel form of cell death was dubbed ferroptosis, which is characterized by iron-dependent accumulation of lipid hydroperoxides that disrupt membrane integrity leading to cell death. Ferroptosis may thus play a key role in the pathogenesis of degenerative diseases in which lipid peroxidation has been implicated. Interestingly, the execution of this form of cell death could be inhibited by the small molecule ferrostatin-1 (Fer-1, **1**).[9] Even though target identification of Fer-1 remains a challenge, the mechanism of action of Fer-1 was recently proposed to derive from its reactivity as a radical-trapping antioxidant.[10]

Unravelling the molecular pathway of ferroptosis is currently a topic of intense study. Because erastin induces ferroptosis through the inhibition of System X_c^-, it can be classified as a class I ferroptosis inducer (FIN). Blockage of this antiporter impairs the cellular uptake of cystine, an essential precursor in the synthesis of the cellular antioxidant glutathione (GSH). The resulting intracellular deficit of GSH in turn triggers the accumulation of ROS, which causes cells to die by excessive oxidation of the membrane lipids (Figure 1).[11] In addition to class I FINs, ferroptosis can also be induced by molecules that directly target and inactivate glutathione peroxidase 4 (GPX4) and are classified as class II FINs.[12,13]

Seiler *et al*. showed that GPX4, a specific type of GSH-dependent selenoprotein, holds an essential role in the antioxidant network of the membranes of a cell. Inducible GPX4-KO significantly increased cell death due to excessive lipid peroxidation, a hallmark feature of ferroptosis.[14] GPX4 has the ability to reduce organic hydroperoxides to the corresponding alcohols while consuming GSH as a reducing agent, further implying the importance of intracellular GSH levels in ferroptosis.[15] Inactivation of GPX4 either directly or indirectly resulted in the accumulation of ROS followed by lipid membrane oxidation which disrupted cell membrane integrity. These findings further solidified GPX4 as a crucial protective enzyme that supresses ferroptosis and it underlines the importance of the GSH-GPX4-axis considering redox homeostasis within the cell membrane (Figure 1).

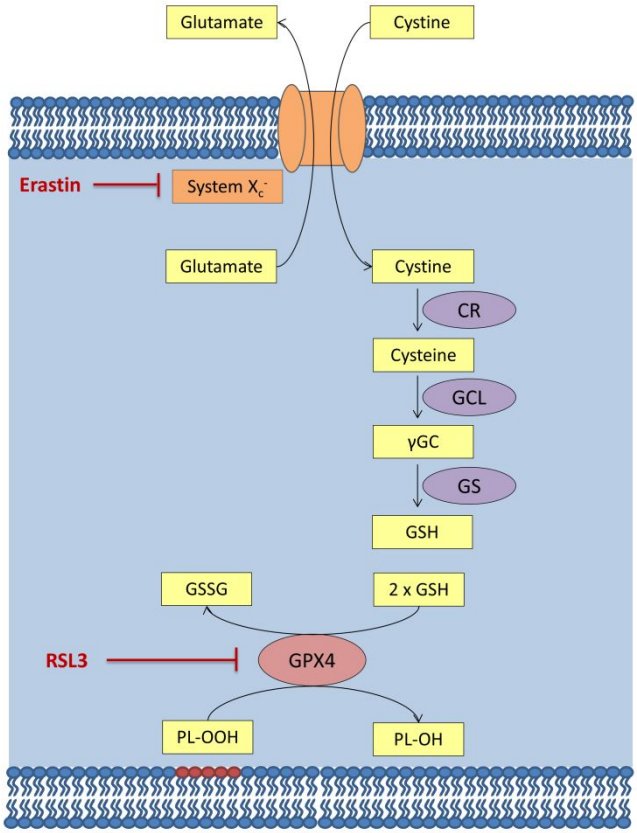

Figure 1. Schematic representation of GPX4-dependent conversion of reactive lipid peroxides to the corresponding lipid alcohols. System X_c^- facilitates the cellular uptake of cystine which is an important precursor in GSH synthesis. Cystine is reduced by cystine reductase (CR) to cysteine. Glutamate cysteine ligase (GCL) attaches a glutamate molecule to cysteine in order to generate γ-glutamyl cysteine (γGC). Addition of a glycine molecule by glutathione synthase (GS) results in the formation of a new molecule of GSH. GSH servers as an important reducing cofactor for GPX4 by catalysing the reduction of lipid peroxides to their corresponding alcohols while also forming glutathione disulfide (GSSG). Erastin inhibits the cellular uptake of cystine and thus impairs intracellular synthesis of GSH. Depletion of GSH leads to the indirect inactivation of GPX4 and the resulting accumulation of lipid peroxides disrupts membrane integrity resulting in ferroptosis. The class II FIN RSL3 acts by directly inactivating GPX4 and does not interfere with the cellular uptake of cystine or intracellular GSH synthesis.[6,16]

The clinical relevance of ferroptosis has been implied in various pathological settings.[17] Dixon *et al*. first showed that Fer-1 was able to prevent glutamate-induced neurotoxicity in a model using organotypic hippocampal slice cultures.[11] Another study in particular showed that ferroptosis might contribute in a whole array of diseases by showing that inhibition of ferroptosis significantly ameliorated the clinical outcome in experimental models for Huntington's disease, periventricular leukomalacia and kidney

dysfunction.[18] Since then multiple studies have implicated an important role of ferroptosis not only in various pathological conditions like ischemia-reperfusion injury[19], neuronal dysfunction[20] and Alzheimer's disease[21], but also in several other biological processes such as hair follicle morphogenesis[22], blood coagulation[23] and in the maturation of photoreceptor cells.[24]

The design of novel and improved ferroptosis inhibitors is thus an interesting field of research. Fer-1 as a lead molecule itself has some unfortunate shortcomings. The presence of a labile ester moiety results in the rapid hydrolysis of Fer-1 into its inactive carboxylic acid. Multiple attempts have been made to improve the potency of this type of molecule while also improving pharmacokinetic parameters of Fer-1 (**2** and **3**, Figure 2).[18,25] While Skouta *et al*. thoroughly explored the structure-activity relationship (SAR) of the Fer-1 scaffold, we previously reported that the replacement of the labile ester moiety of Fer-1 by a more stable sulfonamide group yielded promising results (**4**, UAMC-2418, Figure 2). This intervention significantly improved the metabolic stability while maintaining and even improving potency in a cell-based assay for ferroptosis. These molecules however displayed a poorly soluble character, which limited their use in *in vivo* settings.[16]

In this study, we expand on these earlier findings and we report the synthesis of a novel generation of ferroptosis inhibitors derived from Fer-1 with improved ADME properties and an increased solubility. The pharmacokinetic properties of the most potent molecules were characterized and the *in vivo* efficacy and toxicity of these molecules was investigated. Additionally, a molecular dynamics experiment was conducted as an effort to investigate the binding properties of these molecules in a phospholipid bilayer.

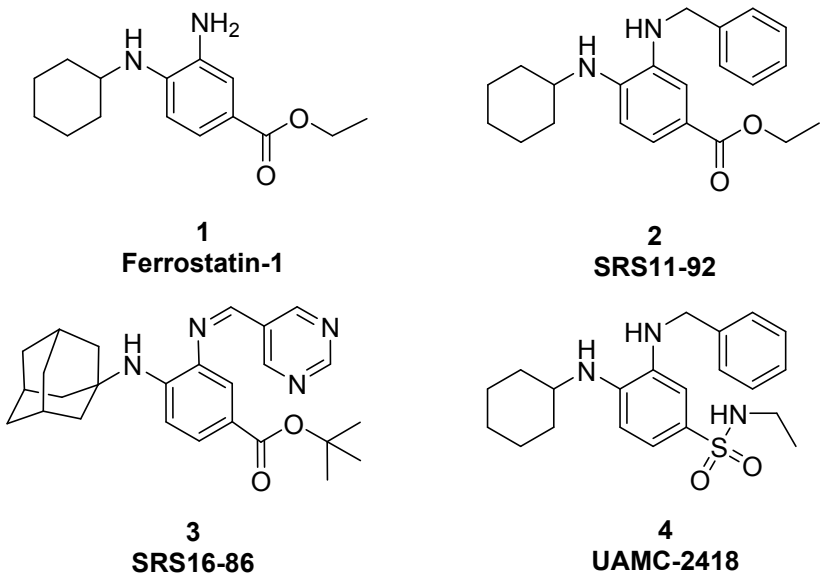

Figure 2. The chemical structure of Ferrostatin-1 and other reported analogues.

RESULTS AND DISCUSSION

Compound design

Our earlier published results involved a thorough exploration of the SAR which provided the following results: (1) The replacement of the labile ester moiety with a sulfonamide greatly improved stability as well as potency (2) The cyclohexyl moiety was deemed to be the most ideal substituent with regard to both potency and lipophilicity. More bulky alkyl groups tend to have a negative effect on the solubility of the compounds and smaller moieties impair the potency of the molecules. (3) The introduction of an aromatic group on the 3-amino position greatly improved potency, but also further decreased the solubility of the compounds.[16]

The major drawback of our previously published molecules was their poor solubility. Designing more soluble compounds is a challenging task since these molecules have to act in the highly lipophilic environment of membranes. We identified that the terminal position of the aliphatic chain on the sulfonamide moiety could be derivatized further in order to increase the solubility of these compounds. A variety of solubility improving groups were introduced at this terminal R_a position. The cyclohexylamine group was kept as in Fer-1 and the R_b position was further derivatized with benzylic and pyridinic substituents in a similar fashion to the previously reported sulfonamide analogues (Figure 3).

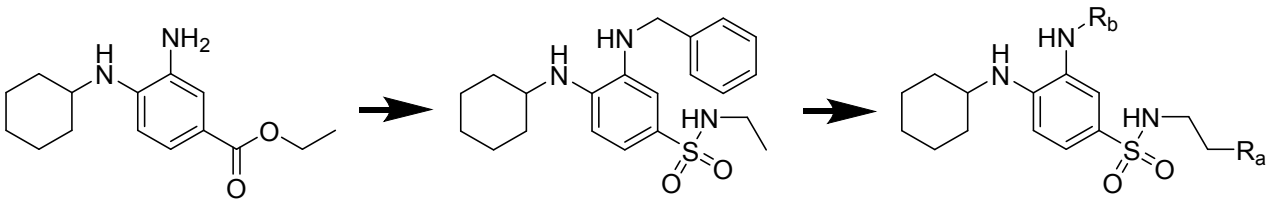

Figure 3. Structural comparison of Fer-1, our previously reported sulfonamide analogue of Fer-1 and the newly synthesized series.

Chemistry

The newly developed series of inhibitors were synthesized according to the general synthetic strategy displayed in Scheme 1.

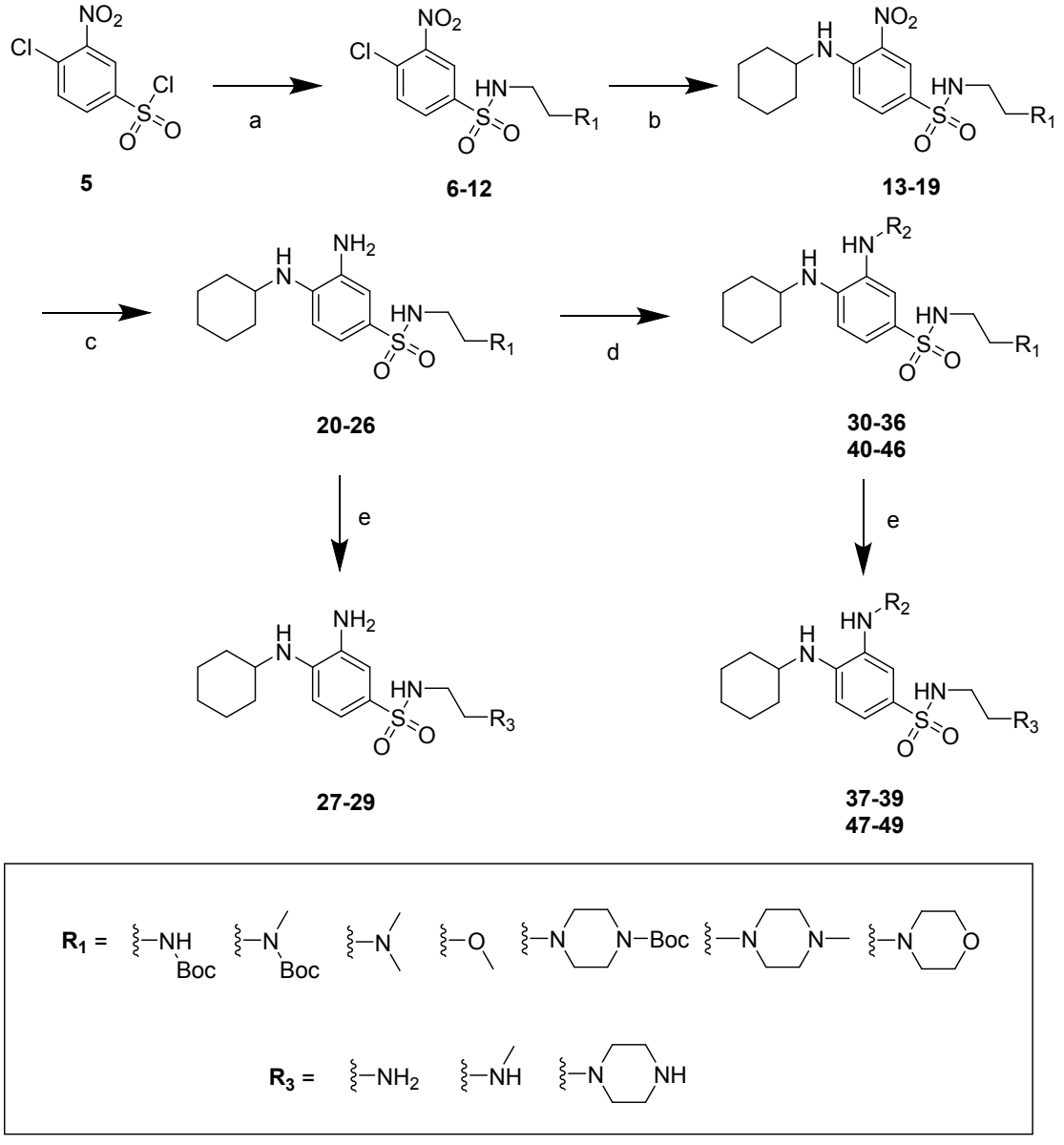

Scheme 1. General overview of the synthetic route.

Reagents and conditions: (a) Aliphatic amine analogue, triethylamine, THF, 1 h, -40°C (b) cyclohexylamine, K_2CO_3 , DMSO, 18 h, 60°C (c) Palladium hydroxide on carbon, H_2, methanol, 18 h, rt (d) benzylbromide or 4-(bromomethyl)pyridine hydrobromide, K_2CO_3, DMF. (e) HCl in dioxane, DCM; in case Boc protection was present.

All molecules were synthesized starting from 4-chloro-3-nitrobenzenesulfonyl chloride **5**. Treatment of **5** with the appropriate amine analogue resulted in the formation of **6-12**. Subsequently a nucleophilic aromatic substitution of **6-12** with cyclohexylamine under basic conditions yielded **13-19**. Palladium-catalysed hydrogenation of the 3-nitro group to its corresponding amine resulted in the generation of molecules **20-26**. Finally, benzylic and pyridinic substituents were introduced at the R_2-position to afford **30-36** and **40-46** respectively. If applicable, the protective Boc group was removed under acidic conditions to yield compounds **27-29**, **37-39** and **47-49**.

Inhibition of Erastin-Induced Ferroptosis *in vitro*

The final set of compounds was evaluated in an assay with IMR-32 neuroblastoma cells in order to assess their potency for inhibiting erastin-induced ferroptosis. In addition to this screening, the kinetic solubility of all newly synthesized molecules was also determined (Table 1) (Additional data such as standard error of the means can be found in the Supporting Information).

The introduction of a cyclic or aliphatic amine at R_1 increased the kinetic solubility of this type of molecule significantly when compared to our earlier published results (Table 1).[16] The introduction of a benzylic moiety at R_2 was well tolerated and improved potency in most cases. Compounds **35-39** for example, all of which contain a benzyl moiety in R_2, displayed a more potent inhibition of erastin-induced ferroptosis than their corresponding analogues which possess a primary amine or pyridinic moiety at this position. This potentiating effect was not observed as significantly when a pyridinic group was introduced at the same position. A similar trend was observed in our previously published work.[16]

For example, compound **35** has an IC_{50}-value of 24 nM combined with a solubility range of 50-100 µM. Even more remarkable is the fact that molecules **37-39** exhibit even lower IC_{50}-values combined with an excellent kinetic solubility (> 200 µM). This increase in solubility while preserving the improved potency when compared to Fer-1 is a very promising feature of these compounds. The four most promising molecules (**35**, **37-39**) were thus selected for further assessment and their *in vitro* ADME-parameters were defined.

Compound	R_1 or R_3	R_2	IC_{50} (nM) [a]	Solubility (µM) [b]
1 (Fer-1)	/	-H	33	> 200
20	$-N(Me)_2$	-H	160	> 200
24	N-Methylpiperazine	-H	236	> 200
25	Morpholine	-H	448	> 200
26	$-OCH_3$	-H	492	> 200

27	-NH(Me)	-H	214	> 200
28	$-NH_2$	-H	306	> 200
29	Piperazine	-H	296	> 200
30	$-N(Me)_2$	Benzyl	554	> 200
34	N-Methylpiperazine	Benzyl	1072	> 200
35	Morpholine	Benzyl	24	50-100
36	$-OCH_3$	Benzyl	22	25-50
37	-NH(Me)	Benzyl	3	> 200
38	$-NH_2$	Benzyl	12	> 200
39	Piperazine	Benzyl	10	> 200
40	$-N(Me)_2$	Pyridinyl	1560	> 200
44	N-Methylpiperazine	Pyridinyl	1520	> 200
45	Morpholine	Pyridinyl	191	> 200
46	$-OCH_3$	Pyridinyl	97	> 200
47	-NH(Me)	Pyridinyl	157	> 200
48	$-NH_2$	Pyridinyl	112	100-200
49	Piperazine	Pyridinyl	442	> 200

Table 1. Synthesized fer-1 analogues and their antiferroptotic activity in response to erastin-induced ferroptosis in IMR-32 Neuroblastoma cells.

[a] Reported IC_{50} values are calculated from measurements in triplicate. Additional information such as the standard error of the means can be found in the Supporting Information.

[b] Final test compound concentration range between 3.125 μM and 200 μM [4 μM DMSO solution in 196 μM buffer solution (10 mM PBS pH 7.4)].

ADME Assays

The determination of both the microsomal and plasma stability of **35**, **37-39** revealed a remarkable improvement in stability when compared to Fer-1 which is unstable under nearly all conditions (Table 2 and Table 3). However, significant intraspecies differences between the four lead molecules were observed. Compounds **38** and **39** more specifically, showed a microsomal half-life ($t_{1/2}$) of multiple hours across all species. Compound **39** has an impressive $t_{1/2}$ when incubated with both human and rat microsomes ($t_{1/2}$ = 20.5 h and $t_{1/2}$ = 16.5 h respectively) but was found to be relatively less stable when incubated with murine microsomes ($t_{1/2}$ = 3.46 h). In contrast, compound **38** has a microsomal $t_{1/2}$ greater than 10 hours under both human ($t_{1/2}$ = 17.7 h) and murine ($t_{1/2}$ = 13 h) conditions but was microsomally less stable when incubated with rat microsomes ($t_{1/2}$ = 2.05 h).

	Microsomal stability ($t_{1/2}$) (h) [a]			**Plasma stability (% recovery after 6h) [b]**		
Compound	**Human**	**Rat**	**Mouse**	**Human**	**Rat**	**Mouse**
1 (Fer-1)	0.109 ± 0.003	0	0	47.3	1.1	0
35 (UAMC-3240)	0.98 ± 0.35	0.173 ± 0.007	0.051 ± 0.002	100	100	100
37 (UAMC-3234)	13.21 ± 4.10	0.35 ± 0.01	0.45 ± 0.02	90.3	65.8	100
38 (UAMC-3206)	17.71 ± 2.04	2.05 ± 0.21	13.00 ± 4.15	100	100	100
39 (UAMC-3203)	20.53 ± 5.49	16.48 ± 4.66	3.46 ± 1.37	84.2	85.8	100

Table 2. Microsomal stability and plasma stability of compounds 1, 35 , 37-39.

[a] Metabolism by microsomes (CYP450 and other NADP-dependent enzymes) was monitored and expressed as half-life (h).

[b] Percentage of remaining parent compound.

	Calculated Intrinsic Clearance *in vitro* (Cl_{int}) (mL/min/kg)		
Compound	**Human**	**Rat**	**Mouse**
35 (UAMC-3240)	22.6 ± 8.1	325.9 ± 13.2	1223.2 ± 48.0
37 (UAMC-3234)	1.7 ± 0.5	161.1 ± 4.6	138.6 ± 6.2
38 (UAMC-3206)	1.3 ± 0.1	27.4 ± 2.7	4.8 ± 1.5
39 (UAMC-3203)	1.1 ± 0.3	3.4 ± 1.0	18.0 ± 7.1

Table 3. Calculated Intrinsic Clearance *in vitro* of compounds 35, 37-39.

The $Cl_{int\ is}$ calculated using the measured microsomal $t_{1/2}$ and takes into account several experimental variables such as the protein concentration and the volume of incubation. The exact formula as well as the species-specific parameters can be found in the Supporting Information.

In vivo evaluation of efficacy of novel fer-1 analogues

We have recently shown that pure cellular iron overload suffices to induce ferroptosis in IMR-32 neuroblastoma cells, which is referred to as non-canonical ferroptosis induction.[26] This new concept of iron-induced ferroptosis has recently been shown by others by using FeCl2 in organotypic hippocampal slice cultures[27], BAY 11-7085 in breast cancer cell lines and glioblastoma[28] and FINO2 in HT1080 fibrosarcoma cells.[29] Both in humans[30] as well as in rodents[31–33], an acute overdose of iron *in vivo* typically results in multiple organ failure and often death.[34,35] First, we have tested the potency of our inhibitors for $(NH_4)_2Fe(SO_4)_2$-induced ferroptosis *in vitro*. Similar to erastin-induced ferroptosis, we found that our most potent inhibitors show similar or lower IC_{50}-values than Fer-1 when inhibiting ferrous ammonium sulphate-induced ferroptosis. (See Supporting Information) Therefore, the selected compounds were assessed for their efficacy in an experimental *in vivo* ferroptosis model using acute iron poisoning. Intravenous injection of compounds **37**, **38** and **39** in mice 15 minutes prior to iron sulphate injection significantly lowered the plasma levels of lactate dehydrogenase (LDH), a general biomarker for organ injury which is drastically elevated in response to iron poisoning. All three compounds were significantly more potent in lowering LDH levels than Fer-1 (Table 4), which illustrates the *in vivo* functionality of these Fer-analogues.

Trigger	Treatment	Plasma LDH (U/L)	Statistics
/	**Vehicle**	484 ± 72	
$FeSO_4$	**Vehicle**	3572 ± 185	
$FeSO_4$	**1 (Fer-1)**	2898 ± 178	* vs. Veh
$FeSO_4$	**37 (UAMC-3234)**	2093 ± 90	**** vs. Veh ** vs. Fer-1
$FeSO_4$	**38 (UAMC-3206)**	2293 ± 148	**** vs. Veh; * vs. Fer-1
$FeSO_4$	**39 (UAMC-3203)**	2346 ± 99	**** vs. Veh; * vs. Fer-1

Table 4. Pretreatment with the compounds significantly decreases LDH levels after acute iron poisoning.

Vehicle, Fer-1 (**1**), compound **37**, **38** or **39** was injected intravenously (20 μmol/kg) 15 minutes before intraperitoneal injection with 300 mg/kg iron sulfate. Two hours after IP injection, mice were sacrificed and blood was taken. Plasma levels of LDH are shown. Vehicle = 2% DMSO in 0.9% NaCl. Error represents SEM, n=5 for twice treated vehicle group, n=11-12 for $FeSO_4$-treated groups. * = 0.01<p< 0.05; ** = 0.001<p<0.01; *** = 0.0001<p<0.001; **** = p < 0.0001. Statistical analysis by ordinary one-way ANOVA.

In vivo pharmacokinetics

In order to estimate how the *in vitro* ADME parameters correlate to an *in vivo* setting, compound **39** (**UAMC-3203**) was selected for a single intravenous (iv) administration to three male Wistar rats at a dose of 5 mg/kg. Blood samples were obtained at various time points (0.083, 0.25, 0.5, 1, 2, 4, and 24h). The concentration of compound **39** was determined using UPLC analysis coupled with tandem quadrupole mass spectrometry. (See Supporting Information) Interestingly, plasma concentrations of compound **39** remained below the detection limit (< 53.1 ng/mL) in nearly all samples. These findings suggest that compound **39** is rapidly removed from the bloodstream and redistributed into various tissues, as can be expected for lipophilic basic compounds.

To assess the extent of tissue distribution of compound **39**, various organs (liver, kidney and lungs) of all three rats were collected on ice at necropsy 24 hours after administration before being homogenized and analysed (Table 5). Significant concentrations of compound **39** were found in all analysed tissues, which further solidifies our earlier findings considering tissue redistribution. Since the tissue concentration of compound **39** was determined 24 hours after iv dosage, these results also confirm the increase in stability when compared to Fer-1 which is unstable in *in vivo* conditions.

	Tissue distribution profile of compound 39 (UAMC-3203) (mg/kg organ, after 24h)		
	Liver	**Kidney**	**Lung**
Rat 1	0.23	0.20	0.19[a]

Rat 2	0.22	0.35	0.48
Rat 3	0.15	0.38	0.53

Table 5. Tissue distribution profile of compound 39 in various organs.

Each rat received an iv dose at 5 mg/kg and the internal organs were collected at necropsy at 24h. The organs were homogenized and further processed by protein precipitation (n=3) and centrifugation. Analysis of the samples was conducted by LC-MS.

[a] For this measurement only two samples of organ homogenate were processed (n=2).

In vivo assessment of toxicity of compound 39

Since ferroptosis plays a role in chronic diseases such as neurodegeneration, we evaluated the toxicity of daily application of compound **39** to wild type mice. Therefore, classic biomarkers of toxicity were measured in blood plasma of mice having received a daily injection of compound **39** over a period of 4 weeks. Plasma alanine aminotransferase (ALT), aspartate aminotransferase (AST), LDH, creatine kinase (CK), creatinine, urea and troponin T levels were all comparable to background values detected in control mice. In addition, no difference in body temperature or weight was observed (Table 6).

Compound	Plasma ALT (U/L)	Plasma AST (U/L)	Plasma LDH (U/L)	Plasma CK (U/L)	Plasma creatinine (mg/dL)	Plasma urea (mg/dL)	Plasma troponin T (µg/L)	Body temperature (°C)	Rel. gain in Body Weight (%)
Vehicle	< 25	110 ± 8	227 ± 18	1501 ± 196	< 0,2	42 ± 2	0,041 ± 0,005	37,0 ± 0,6	14,8 ± 3,4
39 (UAMC-3203)	< 25	123 ± 11	263 ± 20	1865 ± 308	< 0,2	43 ± 2	0,044 ± 0,004	37,0 ± 0,6	10,4 ± 3,3

Table 6. No toxicity was observed in mice after repeated injections of compound 39.

Compound **39** (UAMC-3203) was injected intraperitoneally (20 µmol/kg) daily, over a period of 4 weeks. Body temperature and weight were measured daily, blood parameters were assessed at the 28-day endpoint after sacrifice. Plasma levels of ALT, AST, LDH, CK, creatinine, urea and troponin T are shown. Error represents SEM, n=9/group. Vehicle = 2% DMSO in 0.9% NaCl.

Bilayer insertion of compound 39 occurs on the nanosecond scale

A molecular dynamics study was conceived to investigate the interactions of compound **39** with a model membrane bilayer. The setup consisted of a 128 POPC bilayer in a waterbox. Compound **39** was placed approximately in the centre of the waterbox and allowed to diffuse freely.

A similar system with alpha-tocopherol was included as a reference. Three separate 300 ns simulations were performed for each system. In each of our simulations, compound **39** inserted itself into the lipid bilayer. The solubility-enhancing piperazine ring and the sulphonamide of compound **39** engaged in hydrogen bonding interactions with the phospholipid head groups, while the lipophilic core and ring substituents interacted with the lipid tails (Figure 4A). Comparing compound **39** to the reference compound alpha-tocopherol, it is apparent that compound **39** binds in a more shallow manner than to alpha-tocopherol, which inserts deeply into the membrane (Figure 4B).

The radical-scavenging hydroxyl group of alpha-tocopherol is frequently engaged in hydrogen-bonding interactions to the acyl groups, rendering it unavailable for radical scavenging. By contrast, the aryl amine groups, most prominently the cyclohexylamine group, are less frequently involved in hydrogen bonding.[10,36] This difference in availability may help explain the improved efficacy of compound **39** as a potent ferroptosis inhibitor.

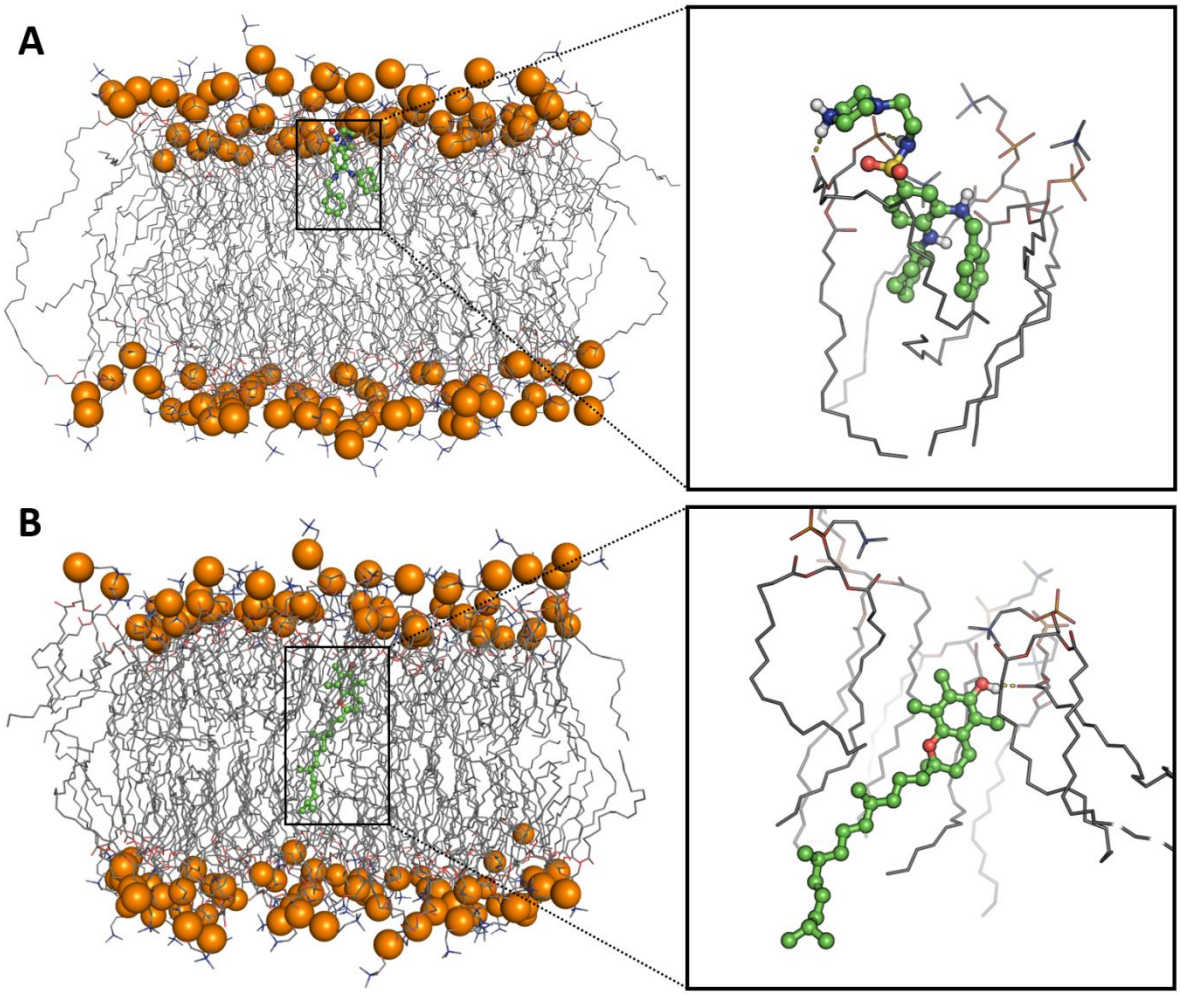

Figure 4. Graphical overview of bilayer insertion of compound **39** and alpha-tocopherol. **(A)** Compound **39** binds in a relatively shallow manner in the phospholipid bilayer. The solubility improving piperazine moiety engages in several hydrogen bonds with the hydrophilic head groups of the phospholipids. **(B)** Alpha-tocopherol binds more deeply in the phospholipid bilayer, while the phenol moiety of the chromanol ring engages in a hydrogen bond interaction with the head group which renders it less suitable for radical scavenging.

CONCLUSION

Fer-1 has traditionally been the most frequently used tool compound in cell death research to inhibit ferroptotic cell death. The use of Fer-1 in multiple *in vitro* settings resulted in a potent dose-dependent inhibition of ferroptosis. Earlier findings suggest that the practical use of Fer-1 *in vivo* is limited due to its poor metabolic stability. Our previously reported research indicated that it was possible to synthesize novel inhibitors of ferroptosis by introducing structural modifications to the Fer-1 scaffold. The elucidation of the SAR of these compounds resulted in a series of sulfonamide derivatives of Fer-1 that were able to inhibit ferroptosis in the single-digit nanomolar range with improved metabolic stability. The major drawback of this series was their poor solubility, preventing them from being used efficiently in *in vivo* settings. In this paper, we report a follow-up series of potent Fer-1 analogues. By introducing both a solubility improving group and a sulfonamide moiety to the Fer-1 scaffold, we were able to synthesize novel molecules that are more potent than Fer-1 while simultaneously improving solubility and stability. Compounds **35**, **37**, **38** and **39** were able to inhibit erastin-induced ferroptotic cell death more potently than Fer-1. These novel compounds were also found to have a significantly improved solubility over our previously published molecules. Additionally, molecules **38** and **39** demonstrate great recovery from plasma after 6h, while also possessing microsomal half-lives of multiple hours across three species. Interestingly, our three most promising compounds (**37, 38** and **39**) were significantly more potent than Fer-1 in protecting against acute iron poisoning induced injury in mice, which illustrate their efficacy *in vivo*. Due to its long microsomal $t_{1/2}$ in rats, compound **39** (UAMC-3203) was selected for single iv dose administration (5 mg/kg) in an effort to estimate the *in vivo* pharmacokinetic properties of these types of molecules. Plasma levels of compound **39** remained below the detection limit in nearly all samples, which implied a rapid redistribution of compound **39** into various tissues. A significant amount of compound **39** was found in liver, kidney and lungs after 24 hours confirming the hypothesis of rapid tissue distribution. No toxicity was observed in mice after daily injection of compound **39** for 4 weeks. Taken together, these findings indicate that these analogues could be used as potent and readily soluble lead compounds to

investigate the process of ferroptotic cell death in various *in vivo* settings or validate their therapeutic value in experimental ferroptosis-driven diseases.

EXPERIMENTAL SECTION

Unless otherwise stated, laboratory reagent grade solvents were used. Reagents were obtained from various commercial sources and were used without any prior purification. Characterization of all compounds was done with ^{1}H and ^{13}C NMR and mass spectrometry of which the spectra were recorded with a 400 MHz Bruker Avance III Nanobay spectrometer with Ultrashield. All obtained spectra were analysed using MestReNova analytical chemistry software. Chemical shifts are displayed in ppm and coupling constants are shown in hertz (Hz). ES mass spectra were obtained from an Esquire 3000plus Ion Trap Mass Spectrometer from Bruker Daltonics. Purities were determined with a HPLC system based either on mass determination or on UV detection. A Waters SQD ESI mass spectrometer was used in combination with a Waters TUV detector. Waters Acquity UPLC BEH C18 1.7 μm, 2.1 mm × 50 mm column was used. The eluens was composed of two different solvents nl. solvent A consisted of water with 0.1% formic acid while solvent B consisted of acetonitrile with 0.1% formic acid. Two methods were used interchangeably on the HPLC system. Method I involved the following parameters: 0.15 min 95% A, 5% B, then in 1.85 min from 95% A, 5% B to 95% B, 5% A, then 0.25 min (0.350 mL/min), 95% B, 5% A. The wavelength for UV detection was 254 nm. Method II involved the following: flow 0.4 mL/min, 0.25 min 95% A, 5% B, then in 4.75 min to 95% B, 5% A, then 0.25 min 95% B, 5% A, followed by 0.75 min 95% A, 5% B. The wavelength for UV detection was 214 nm. During the chemical synthesis, flash purification was performed when necessary on a Biotage ISOLERA One flash system equipped with an internal variable dual wavelength diode array detector (200−400 nm). For normal phase purifications SNAP cartridges (10−340 g, flow rate of 10−100 mL/min) were used, and reversed phase purifications were done while using of KP-C18 containing cartridges. Dry sample loading was done by self-packing samplet cartridges using silica and Celite® 545, respectively, for normal and reversed phase purifications. Gradients used varied for each purification. During the pharmacokinetic characterization, mouse and rat plasma were obtained from Innovative Research. Liver microsomes were purchased from Corning B.V.

Life Sciences. The turbidity in the kinetic solubility experiments was measured using the UV/VIS spectrophotometer Synergy MX, Biotek with Gen5.

The following section comprises the synthetic procedures and analytical data for all compounds reported in this manuscript. Several synthetic procedures that were used in the preparation of intermediates and final products are summarized here as "General Procedures". The purities of all final products were found to be > 95%, unless stated otherwise.

General procedure A

A solution containing the appropriate aliphatic or cyclic amine substituent (1 equiv.) and triethylamine (2 equiv.) in THF was added dropwise to a solution containing 4-chloro-3-nitrobenzene-1-sulfonyl chloride **5** (1 equiv.) in THF that was cooled down to -40°C. After the addition was complete, the resulting mixture was allowed to warm up to room temperature over the course of one hour. Subsequently the reaction mixture was diluted with EtOAc and washed three times with water. The organic layer was dried using anhydrous sodium sulphate before being concentrated *in vacuo*. The crude reaction products **6-12** were used without any further purification.

General procedure B

Intermediates **6-12** (1 equiv.) were dissolved in DMSO before potassium carbonate (2 equiv.) and cyclohexanamine (1.2 equiv.) were added. The resulting mixture was heated to a temperature of 60°C and then stirred overnight. After cooling down to room temperature, the reaction mixture was diluted with EtOAc and washed three times with water. The organic layer was dried using anhydrous sodium sulphate before being concentrated *in vacuo*. If deemed necessary, further purification was conducted with flash chromatography on silica gel using a gradient consisting of heptanes and EtOAc to obtain intermediates **13-19**.

General procedure C

Intermediates **13-19** (1 equiv.) were dissolved in dry MeOH and the solution was purged using argon gas. Palladium(II) hydroxide was added under inert atmosphere while continuously stirring. After the addition was complete, the resulting mixture was put under hydrogen atmosphere and left to stir overnight. The reaction mixture was filtered through a patch of Celite® and then purified by flash chromatography on silica gel using a gradient consisting of heptanes and EtOAc to yield products **20-26**.

General procedure D

Compounds **20-26** (1 equiv.) were dissolved in DMF followed by the addition of potassium carbonate (1 – 3 equiv.) and the corresponding benzyl- or pyridinylderivate (1-2 equiv.). This mixture was allowed to stir at various temperatures and timespans, all of which are further specified at the corresponding compounds reported below. The crude product was then purified by either normal phase or reversed phase flash chromatography to yield compounds **30-36** and **40-46**. The exact conditions of these purifications are reported below for each compound individually.

General procedure E

Compounds **21-23**, **31-33** and **41-43** (1 equiv.) were dissolved in dichloromethane followed by the addition of a 4M solution of hydrochloric acid in dioxane (8 equiv.) The reaction mixture was stirred at room temperature for 2 hours. After reaction diethylether was added to the reaction mixture in order to precipitate compounds **27-29**, **37-39** and **47-49**. The obtained HCl-salts were subsequently washed with a minimal amount of diethylether.

4-chloro-N-(2-(dimethylamino)ethyl)-3-nitrobenzenesulfonamide (6)

By following **General Procedure A** and using N,N-dimethylethane-1,2-diamine (1.38 g, 15.62 mmol) as the corresponding amine, the formation of 4-chloro-N-(2-(dimethylamino)ethyl)-3-nitrobenzenesulfonamide **6** (4.67 g, 15.16 mmol) was achieved. (Yield: 97%)

^{1}H NMR (400 MHz, DMSO-d_6) δ 2.07 (s, 6H), 2.25 - 2.30 (m, 2H), 2.97 (t, J = 6.5 Hz, 2H), 8.05 (d, J = 8.5 Hz, 1H), 8.12 (dd, J = 8.5, 2.2 Hz, 1H), 8.50 (d, J = 2.1 Hz, 1H).

^{13}C NMR (101 MHz, DMSO-d_6) δ 40.62, 44.83, 58.06, 123.88, 128.93, 131.23, 132.84, 141.20, 147.31.

tert-butyl (2-((4-chloro-3-nitrophenyl)sulfonamido)ethyl)(methyl)carbamate (7)

By following **General Procedure A** and using tert-butyl (2-aminoethyl)(methyl)carbamate (2.04 g, 11.72 mmol) as the corresponding amine, the formation of tert-butyl (2-((4-chloro-3-nitrophenyl)sulfonamido)ethyl)(methyl)carbamate **7** (4.58 g, 11.62 mmol) was achieved. (Yield: 99%)

^{1}H NMR (400 MHz, Acetone-d_6) δ 1.42 (s, 9H), 2.83 (d, J = 14.4 Hz, 3H), 3.20 (t, J = 6.3 Hz, 2H), 3.31 - 3.42 (m, 2H), 7.03 (s, 1H), 8.00 (d, J = 8.4 Hz, 1H), 8.15 (dd, J = 8.5, 2.2 Hz, 1H), 8.45 (d, J = 2.2 Hz, 1H).

^{13}C NMR (101 MHz, Acetone-d_6) δ 27.64, 41.25, 47.95, 48.67, 78.86, 124.14, 124.22, 129.91, 131.38, 133.07, 141.36, 148.03.

tert-butyl (2-((4-chloro-3-nitrophenyl)sulfonamido)ethyl)carbamate (8)

By following **General Procedure A** and using tert-butyl (2-aminoethyl)carbamate (3.28 g, 20.5 mmol) as the correspoding amine, the formation of tert-butyl (2-((4-chloro-3-nitrophenyl)sulfonamido)ethyl)carbamate **8** (6.2 g, 16.32 mmol) was achieved (Yield: 84%)

^{1}H NMR (400 MHz, Acetone-d_6) δ 1.37 (s, 9H), 3.09 - 3.17 (m, 2H), 3.17 - 3.23 (m, 2H), 6.11 (t, J = 6.0 Hz, 1H), 7.02 (t, J = 5.7 Hz, 1H), 7.97 (d, J = 8.5 Hz, 1H), 8.14 (dd, J = 8.4, 2.2 Hz, 1H), 8.44 (d, J = 2.2 Hz, 1H).

^{13}C NMR (101 MHz, Acetone-d_6) δ 27.74, 40.11, 43.17, 78.29, 124.27, 130.01, 131.43, 133.08, 141.28, 147.95, 156.09.

tert-butyl 4-(2-((4-chloro-3-nitrophenyl)sulfonamido)ethyl)piperazine-1-carboxylate (9)

By following **General Procedure A** and using 4-*N*-(2-Aminoethyl)-1-*N*-Boc-piperazine (3.76 g, 16.4 mmol) as the correspoding amine, the formation of tert-butyl 4-(2-((4-chloro-3-nitrophenyl)sulfonamido)ethyl)piperazine-1-carboxylate **9** (6.7 g, 16.32 mmol) was achieved (Yield: 96%)

^{1}H NMR (400 MHz, DMSO-d_6) δ 1.38 (s, 9H), 2.22 (t, J = 5.0 Hz, 4H), 2.32 (t, J = 6.5 Hz, 2H), 2.98 (q, J = 5.3 Hz, 2H), 3.20 (dd, J = 6.3, 3.6 Hz, 4H), 7.98 - 8.05 (m, 2H), 8.08 (dd, J = 8.5, 2.1 Hz, 1H), 8.46 (d, J = 2.1 Hz, 1H).

^{13}C NMR (101 MHz, DMSO-d_6) δ 28.00, 43.05, 52.23, 56.69, 78.70, 123.82, 129.01, 131.24, 132.96, 141.12, 147.40, 153.72.

4-chloro-N-(2-(4-methylpiperazin-1-yl)ethyl)-3-nitrobenzenesulfonamide (10)

By following **General Procedure A** and using 2-(4-methylpiperazin-1-yl)ethanamine (2.24 g, 15.16 mmol) as the corresponding amine, the formation of 4-chloro-N-(2-(4-methylpiperazin-1-yl)ethyl)-3-nitrobenzenesulfonamide **10** (5.13 g, 14.14 mmol) was achieved. (Yield: 91%)

^{1}H NMR (400 MHz, DMSO-d_6) δ 2.09 (s, 3H), 2.12 - 2.26 (m, 8H), 2.29 (t, J = 6.5 Hz, 2H), 2.97 (t, J = 6.5 Hz, 2H), 8.02 (d, J = 8.5 Hz, 1H), 8.08 (dd, J = 8.5, 2.1 Hz, 1H), 8.45 (d, J = 2.1 Hz, 1H).

^{13}C NMR (101 MHz, DMSO-d_6) δ 40.03, 45.63, 52.40, 54.39, 56.86, 123.81, 128.96, 131.21, 132.91, 141.33, 147.38.

4-chloro-N-(2-morpholinoethyl)-3-nitrobenzenesulfonamide (11)

By following **General Procedure A** and using 2-morpholinoethanamine (2.054 mL, 15.62 mmol) as the corresponding amine, the formation of 4-chloro-N-(2-morpholinoethyl)-3-nitrobenzenesulfonamide **11** (5.17 g, 14.78 mmol) was achieved. (Yield: 95%)

^{1}H NMR (400 MHz, DMSO-d_6) δ 2.22 - 2.27 (m, 4H), 2.30 (t, J = 6.5 Hz, 2H), 2.93 - 3.02 (m, 2H), 3.43 - 3.48 (m, 4H), 8.02 (s, 1H), 8.03 (d, J = 8.3 Hz, 1H), 8.08 (dd, J = 8.5, 2.1 Hz, 1H), 8.46 (d, J = 2.1 Hz, 1H).

^{13}C NMR (101 MHz, DMSO-d_6) δ 40.09, 52.99, 57.18, 65.92, 123.83, 128.99, 131.23, 132.94, 141.17, 147.39.

4-chloro-N-(2-methoxyethyl)-3-nitrobenzenesulfonamide (12)

By following **General Procedure A** and using 2-methoxyethanamine (1.42 g, 16.4 mmol) as the correspoding amine, the formation of 4-chloro-N-(2-methoxyethyl)-3-nitrobenzenesulfonamide **12** (4.2 g, 14.25 mmol) was achieved (Yield: 91%)

^{1}H NMR (400 MHz, Acetone-d_6) δ 3.18 (s, 3H), 3.22 (t, J = 5.3 Hz, 2H), 3.38 - 3.45 (m, 2H), 6.86 (s, 1H), 7.93 (d, J = 8.5 Hz, 1H), 8.14 (dd, J = 8.5, 2.2 Hz, 1H), 8.44 (d, J = 2.2 Hz, 1H).

^{13}C NMR (101 MHz, Acetone-d_6) δ 42.95, 57.83, 70.75, 124.28, 129.97, 131.50, 132.95, 141.48, 147.79.

4-(cyclohexylamino)-N-(2-(dimethylamino)ethyl)-3-nitrobenzenesulfonamide (13)

By following **General Procedure B** and using 4-chloro-N-(2-(dimethylamino)ethyl)-3-nitrobenzenesulfonamide **6** (4.665 g, 15.16 mmol) as the staring material, the formation of 4-(cyclohexylamino)-N-(2-(dimethylamino)ethyl)-3-nitrobenzenesulfonamide **13** (4.72 g, 12.74 mmol) was achieved. (Yield: 84%)

^{1}H NMR (400 MHz, DMSO-d_6) δ 1.26 - 1.32 (m, 1H), 1.41 - 1.51 (m, 4H), 1.61 - 1.68 (m, 1H), 1.71 - 1.80 (m, 2H), 1.96 - 2.03 (m, 2H), 2.09 (s, 6H), 2.29 (t, J = 6.8 Hz, 2H), 2.85 (t, J = 6.8 Hz, 2H), 3.70 -

3.81 (m, 1H), 7.36 (d, J = 9.3 Hz, 1H), 7.85 (dd, J = 9.2, 2.3, 0.7 Hz, 1H), 8.32 (d, J = 7.8 Hz, 1H), 8.49 (d, J = 2.3 Hz, 1H).

^{13}C NMR (101 MHz, DMSO-d_6) δ 23.97, 24.92, 31.72, 40.58, 45.00, 50.63, 58.02, 115.89, 126.04, 126.17, 129.47, 133.34, 145.80.

tert-butyl (2-((4-(cyclohexylamino)-3-nitrophenyl)sulfonamido)ethyl)(methyl)carbamate (14)

By following **General Procedure B** and using tert-butyl (2-((4-chloro-3-nitrophenyl)sulfonamido)ethyl)(methyl)carbamate **7** (4.58 g, 11.62 mmol) as the starting material, the formation of tert-butyl (2-((4-(cyclohexylamino)-3-nitrophenyl)sulfonamido)ethyl)(methyl)carbamate **14** (3.46 g, 7.58 mmol) was achieved. (Yield: 65%)

^{1}H NMR (400 MHz, DMSO-d_6) δ 1.22 - 1.30 (m, 1H), 1.36 (s, 9H), 1.39 - 1.48 (m, 4H), 1.56 - 1.65 (m, 1H), 1.71 (dd, J = 9.1, 4.7 Hz, 2H), 1.92 - 2.01 (m, 2H), 2.75 (s, 3H), 2.85 (t, J = 6.7 Hz, 2H), 3.18 (t, J = 6.7 Hz, 2H), 3.68 - 3.79 (m, 1H), 7.32 (d, J = 9.2 Hz, 1H), 7.69 (s, 1H), 7.78 (dd, J = 9.3, 2.3 Hz, 1H), 8.28 (d, J = 7.8 Hz, 1H), 8.44 (d, J = 2.3 Hz, 1H).

^{13}C NMR (101 MHz, DMSO-d_6) δ 24.44, 25.41, 28.45, 32.22, 41.02, 48.73, 51.16, 79.04, 116.52, 126.49, 126.54, 130.08, 133.74, 146.37, 155.07.

tert-butyl (2-((4-(cyclohexylamino)-3-nitrophenyl)sulfonamido)ethyl)carbamate (15)

By following **General Procedure B** and using tert-butyl (2-((4-chloro-3-nitrophenyl)sulfonamido)ethyl)carbamate **8** (3 g, 7.90 mmol) as the starting material, the formation of tert-butyl (2-((4-(cyclohexylamino)-3-nitrophenyl)sulfonamido)ethyl)carbamate **15** (3.3 g, 7.46 mmol) was achieved. (Yield: 94%)

^{1}H NMR (400 MHz, Acetone-d_6) δ 1.24 - 1.33 (m, 1H), 1.37 (s, 9H), 1.43 - 1.58 (m, 4H), 1.62 - 1.72 (m, 1H), 1.72 - 1.84 (m, 2H), 2.07 - 2.13 (m, 2H), 2.79 (s, 1H), 3.01 (q, J = 6.3 Hz, 2H), 3.17 (q, J = 6.0 Hz,

2H), 6.03 (s, 1H), 6.58 (t, J = 6.1 Hz, 1H), 7.29 (dd, J = 9.4, 2.9 Hz, 1H), 7.84 (dd, J = 9.2, 2.4 Hz, 1H), 8.37 (d, J = 7.7 Hz, 1H), 8.56 (d, J = 2.4 Hz, 1H).

^{13}C NMR (101 MHz, Acetone-*d_6*) δ 24.24, 25.23, 27.66, 32.19, 40.07, 43.11, 51.19, 78.04, 115.56, 126.51, 126.69, 130.33, 133.45, 146.34, 155.96.

tert-butyl 4-(2-((4-(cyclohexylamino)-3-nitrophenyl)sulfonamido)ethyl)piperazine-1-carboxylate (16)

By following **General Procedure B** and using tert-butyl 4-(2-((4-chloro-3-nitrophenyl)sulfonamido)ethyl)piperazine-1-carboxylate **9** (6.7 g, 14.92 mmol) as the starting material, the formation of tert-butyl 4-(2-((4-(cyclohexylamino)-3-nitrophenyl)sulfonamido)ethyl)piperazine-1-carboxylate **16** (6.5 g, 12.7 mmol) was achieved. (Yield: 85%)

^{1}H NMR (400 MHz, DMSO-*d_6*) δ 1.38 (s, 9H), 1.40 - 1.47 (m, 5H), 1.56 - 1.65 (m, 1H), 1.68 - 1.77 (m, 2H), 1.92 - 1.99 (m, 2H), 2.22 (t, J = 5.0 Hz, 4H), 2.32 (t, J = 6.7 Hz, 2H), 2.86 (t, J = 6.7 Hz, 2H), 3.22 (t, J = 5.0 Hz, 4H), 3.73 (d, J = 9.3 Hz, 1H), 7.22 (s, 1H), 7.33 (d, J = 9.3 Hz, 1H), 7.81 (ddd, J = 9.3, 2.3, 0.7 Hz, 1H), 8.29 (d, J = 7.8 Hz, 1H), 8.44 (d, J = 2.2 Hz, 1H).

^{13}C NMR (101 MHz, DMSO-*d_6*) δ 23.97, 24.91, 28.00, 31.71, 42.79, 50.63, 52.29, 56.58, 78.66, 115.95, 126.04, 126.17, 129.48, 133.36, 145.81, 153.70.

4-(cyclohexylamino)-N-(2-(4-methylpiperazin-1-yl)ethyl)-3-nitrobenzenesulfonamide (17)

By following **General Procedure B** and using 4-chloro-N-(2-(4-methylpiperazin-1-yl)ethyl)-3-nitrobenzenesulfonamide **10** (5.1 g, 14.06 mmol) as the starting material, the formation of 4-(cyclohexylamino)-N-(2-(4-methylpiperazin-1-yl)ethyl)-3-nitrobenzenesulfonamide **17** (5.04 g, 11.84 mmol) was achieved. (Yield: 84%)

^{1}H NMR (400 MHz, DMSO-*d_6*) δ 1.21 - 1.31 (m, 1H), 1.37 - 1.47 (m, 4H), 1.57 - 1.65 (m, 1H), 1.67 - 1.76 (m, 2H), 1.91 - 1.99 (m, 2H), 2.09 (s, 3H), 2.12 - 2.26 (m, 8H), 2.29 (t, J = 6.8 Hz, 2H), 2.84 (t, J =

6.7 Hz, 2H), 3.68 - 3.78 (m, 1H), 7.31 (d, J = 9.4 Hz, 1H), 7.80 (dd, J = 9.2, 2.3, 0.6 Hz, 1H), 8.29 (d, J = 7.8 Hz, 1H), 8.43 (d, J = 2.3 Hz, 1H).

^{13}C NMR (101 MHz, DMSO-d_6) δ 23.96, 24.91, 31.73, 40.03, 45.69, 50.62, 52.51, 54.50, 56.77, 115.90, 126.03, 126.27, 129.50, 133.33, 145.81.

4-(cyclohexylamino)-N-(2-morpholinoethyl)-3-nitrobenzenesulfonamide (18)

By following **General Procedure B** and using 4-chloro-N-(2-morpholinoethyl)-3-nitrobenzenesulfonamide **11** (5.13 g, 14.66 mmol) as the starting material, the formation of 4-(cyclohexylamino)-N-(2-morpholinoethyl)-3-nitrobenzenesulfonamide **18** (5.3 g, 12.85 mmol) was achieved. (Yield: 88%)

^{1}H NMR (400 MHz, DMSO-d_6) δ 1.21 - 1.32 (m, 1H), 1.36 - 1.48 (m, 4H), 1.57 - 1.65 (m, 1H), 1.66 - 1.76 (m, 2H), 1.90 - 1.99 (m, 2H), 2.23 - 2.28 (m, 4H), 2.30 (t, J = 6.7 Hz, 2H), 2.85 (t, J = 6.7 Hz, 2H), 3.49 (t, J = 4.6 Hz, 4H), 3.69 - 3.77 (m, 1H), 7.32 (d, J = 9.3 Hz, 1H), 7.81 (dd, J = 9.1, 2.2, 0.6 Hz, 1H), 8.29 (d, J = 7.8 Hz, 1H), 8.44 (d, J = 2.3 Hz, 1H).

^{13}C NMR (101 MHz, DMSO-d_6) δ 23.97, 24.92, 31.71, 40.11, 50.63, 53.08, 57.11, 66.00, 115.94, 126.05, 126.15, 129.48, 133.33, 145.81.

4-(cyclohexylamino)-N-(2-methoxyethyl)-3-nitrobenzenesulfonamide (19)

By following **General Procedure B** and using 4-chloro-N-(2-methoxyethyl)-3-nitrobenzenesulfonamide **12** (3 g, 10.18 mmol) as the starting material, the formation of 4-(cyclohexylamino)-N-(2-methoxyethyl)-3-nitrobenzenesulfonamide **19** (2.27 g, 6.36 mmol) was achieved. (Yield: 62.5%)

^{1}H NMR (400 MHz, DMSO-d_6) δ 1.18 - 1.33 (m, 1H), 1.36 - 1.51 (m, 4H), 1.54 - 1.66 (m, 1H), 1.67 - 1.78 (m, 2H), 1.88 - 2.04 (m, 2H), 2.90 (q, J = 5.6 Hz, 2H), 3.17 (s, 3H), 3.29 - 3.31 (m, 2H), 3.66 - 3.80 (m, 1H), 7.31 (d, J = 9.3 Hz, 1H), 7.69 (t, J = 5.8 Hz, 1H), 7.80 (dd, J = 9.2, 2.3 Hz, 1H), 8.27 (d, J = 7.8 Hz, 1H), 8.44 (d, J = 2.2 Hz, 1H).

^{13}C NMR (101 MHz, DMSO-d_6) δ 24.45, 25.42, 32.23, 42.61, 51.14, 58.33, 70.98, 116.39, 126.53, 126.79, 130.03, 133.82, 146.33.

3-amino-4-(cyclohexylamino)-N-(2-(dimethylamino)ethyl)benzenesulfonamide (20)

By following **General Procedure C** and using 4-(cyclohexylamino)-N-(2-(dimethylamino)ethyl)-3-nitrobenzenesulfonamide **13** (4.72 g, 12.74 mmol) as the starting material, 3-amino-4-(cyclohexylamino)-N-(2-(dimethylamino)ethyl)benzenesulfonamide **20** (2.2 g, 6.46 mmol) was generated. (Yield: 51%)

^{1}H NMR (400 MHz, DMSO-d_6) δ 1.13 - 1.25 (m, 3H), 1.29 - 1.43 (m, 2H), 1.63 (dt, J = 12.6, 3.6 Hz, 1H), 1.74 (dt, J = 13.2, 3.7 Hz, 2H), 1.92 - 1.99 (m, 2H), 2.06 (s, 6H), 2.23 (t, 2H), 2.70 - 2.75 (m, 2H), 3.24 - 3.33 (m, 1H), 4.85 (d, J = 7.5 Hz, 1H), 4.95 (s, 2H), 6.50 (d, J = 9.0 Hz, 1H), 6.81 - 6.86 (m, 1H), 6.90 - 6.95 (m, 2H).

^{13}C NMR (101 MHz, DMSO-d_6) δ 24.66, 25.55, 32.53, 40.63, 45.08, 50.69, 58.00, 107.91, 111.49, 117.19, 125.77, 134.44, 138.06.

t_R 1.32 min, MS (ESI) m/z 341 [M +H] (100%)

tert-butyl (2-((3-amino-4-(cyclohexylamino)phenyl)sulfonamido)ethyl)(methyl)carbamate (21)

By following **General Procedure C** and using tert-butyl (2-((4-(cyclohexylamino)-3-nitrophenyl)sulfonamido)ethyl)(methyl)carbamate **14** (3.46 g, 7.58 mmol) as starting material, tert-butyl (2-((3-amino-4-(cyclohexylamino)phenyl)sulfonamido)ethyl)(methyl)carbamate **21** (1.98 g, 4.64 mmol) was generated. (Yield: 61.2%)

^{1}H NMR (400 MHz, DMSO-d_6) δ 1.13 - 1.27 (m, 3H), 1.33 - 1.40 (m, 11H), 1.63 (dt, J = 12.7, 3.7 Hz, 1H), 1.74 (dt, J = 13.3, 3.6 Hz, 2H), 1.92 - 2.00 (m, 2H), 2.71 - 2.80 (m, 5H), 3.15 (t, J = 6.9 Hz, 2H), 3.23 - 3.33 (m, 1H), 4.86 (d, J = 7.5 Hz, 1H), 4.96 (s, 2H), 6.50 (d, J = 8.9 Hz, 1H), 6.90 - 6.95 (m, 2H), 7.11 (s, 1H).

^{13}C NMR (101 MHz, DMSO-d_6) δ 24.66, 25.55, 27.99, 32.52, 34.83, 40.66, 48.24, 50.68, 78.51, 107.86, 111.38, 117.14, 125.72, 134.48, 138.09, 154.57.

tert-butyl (2-((3-amino-4-(cyclohexylamino)phenyl)sulfonamido)ethyl)carbamate (22)

By following **General Procedure C** and using tert-butyl (2-((4-(cyclohexylamino)-3-nitrophenyl)sulfonamido)ethyl)carbamate **15** (2.7 g, 6.1 mmol) as starting material, tert-butyl (2-((3-amino-4-(cyclohexylamino)phenyl)sulfonamido)ethyl)carbamate **22** (1.5 g, 3.64 mmol) was generated. (Yield: 59.6%)

^{1}H NMR (400 MHz, DMSO-d_6) δ 1.15 - 1.27 (m, 3H), 1.36 (s, 11H), 1.55 - 1.68 (m, 1H), 1.70 - 1.78 (m, 2H), 1.92 - 2.03 (m, 2H), 2.67 (q, J = 6.6, 6.1 Hz, 2H), 2.95 (q, J = 6.7 Hz, 2H), 3.24 - 3.30 (m, 1H), 4.83 (d, J = 7.5 Hz, 1H), 4.93 (s, 2H), 6.50 (d, J = 8.8 Hz, 1H), 6.71 (d, J = 6.4 Hz, 1H), 6.88 - 6.94 (m, 2H), 6.97 - 7.05 (m, 1H).

^{13}C NMR (101 MHz, DMSO-d_6) δ 25.15, 26.04, 28.66, 31.78, 33.05, 42.87, 51.22, 78.20, 108.42, 111.97, 117.68, 126.27, 134.95, 138.65, 155.95**.**

tert-butyl 4-(2-((3-amino-4-(cyclohexylamino)phenyl)sulfonamido)ethyl)piperazine-1-carboxylate (23)

By following **General Procedure C** and using tert-butyl 4-(2-((4-(cyclohexylamino)-3-nitrophenyl)sulfonamido)ethyl)piperazine-1-carboxylate **16** (6.5 g, 12.7 mmol) as starting material, tert-butyl 4-(2-((3-amino-4-(cyclohexylamino)phenyl)sulfonamido)ethyl)piperazine-1-carboxylate **23** (3.9 g, 8.1 mmol) was generated. (Yield: 63.7%)

^{1}H NMR (400 MHz, DMSO-d_6) δ 1.12 - 1.27 (m, 3H), 1.29 - 1.36 (m, 2H), 1.39 (s, 9H), 1.58 - 1.68 (m, 1H), 1.68 - 1.78 (m, 2H), 1.90 - 2.01 (m, 2H), 2.21 (t, J = 5.3 Hz, 4H), 2.30 (dd, J = 7.7, 6.2 Hz, 2H), 2.77 (dt, J = 7.7, 6.0 Hz, 2H), 3.24 (t, J = 5.1 Hz, 4H), 3.27 - 3.32 (m, 1H), 4.85 (d, J = 7.5 Hz, 1H), 4.95 (s, 2H), 6.50 (d, J = 9.0 Hz, 1H), 6.81 (t, J = 5.8 Hz, 1H), 6.93 (dq, J = 4.3, 2.2 Hz, 2H).

^{13}C NMR (101 MHz, DMSO-d_6) δ 24.65, 25.55, 28.01, 30.65, 32.52, 42.98, 50.70, 52.33, 56.54, 78.65, 107.92, 111.50, 117.24, 125.69, 134.47, 138.09, 153.71.

3-amino-4-(cyclohexylamino)-N-(2-(4-methylpiperazin-1-yl)ethyl)benzenesulfonamide (24)

By following **General Procedure C** and using 4-(cyclohexylamino)-N-(2-(4-methylpiperazin-1-yl)ethyl)-3-nitrobenzenesulfonamide **17** (5.0 g, 11.75 mmol) as starting material, 3-amino-4-(cyclohexylamino)-N-(2-(4-methylpiperazin-1-yl)ethyl)benzenesulfonamide **24** (3.00 g, 7.58 mmol) was generated. (Yield: 64.5%)

^{1}H NMR (400 MHz, DMSO-d_6) δ 1.11 - 1.26 (m, 3H), 1.29 - 1.43 (m, 2H), 1.58 - 1.67 (m, 1H), 1.69 - 1.78 (m, 2H), 1.93 - 1.99 (m, 2H), 2.11 (s, 3H), 2.14 - 2.35 (m, 10H), 2.68 - 2.77 (m, 2H), 3.23 - 3.34 (m, 1H), 4.86 (d, J = 7.5 Hz, 1H), 4.96 (s, 2H), 6.49 (d, J = 9.0 Hz, 1H), 6.81 (t, J = 5.8 Hz, 1H), 6.90 - 6.94 (m, 2H).

^{13}C NMR (101 MHz, DMSO-d_6) δ 24.66, 25.55, 32.52, 40.10, 45.71, 50.68, 52.53, 54.59, 56.67, 107.90, 111.46, 117.19, 125.63, 134.45, 138.06.

t_R 1.29 min, MS (ESI) m/z 396 [M +H] (100%)

3-amino-4-(cyclohexylamino)-N-(2-morpholinoethyl)benzenesulfonamide (25)

By following **General Procedure C** and using 4-(cyclohexylamino)-N-(2-morpholinoethyl)-3-nitrobenzenesulfonamide **18** (5.3 g, 12.85 mmol) as starting material, 3-amino-4-(cyclohexylamino)-N-(2-morpholinoethyl)benzenesulfonamide **25** (3.4 g, 8.89 mmol) was generated. (Yield: 69.2%)

^{1}H NMR (400 MHz, DMSO-d_6) δ 1.13 - 1.28 (m, 3H), 1.29 - 1.43 (m, 2H), 1.63 (dt, J = 12.5, 3.8 Hz, 1H), 1.70 - 1.79 (m, 2H), 1.92 - 1.99 (m, 2H), 2.23 - 2.32 (m, 6H), 2.77 (dt, J = 7.6, 5.9 Hz, 2H), 3.23 - 3.34 (m, 1H), 3.49 - 3.52 (m, 4H), 4.84 (d, J = 7.5 Hz, 1H), 4.95 (s, 2H), 6.50 (d, J = 9.0 Hz, 1H), 6.82 (t, J = 11.7, 5.9 Hz, 1H), 6.92 - 6.95 (m, 2H).

^{13}C NMR (101 MHz, DMSO-d_6) δ 24.65, 25.55, 32.52, 39.79, 50.69, 53.12, 57.06, 66.06, 107.90, 111.51, 117.24, 125.68, 134.46, 138.10.

t_R 1.31 min, MS (ESI) m/z 383 [M +H] (100%)

3-amino-4-(cyclohexylamino)-N-(2-methoxyethyl)benzenesulfonamide (26)

By following **General Procedure C** and using 4-(cyclohexylamino)-N-(2-methoxyethyl)-3-nitrobenzenesulfonamide **19** (3.5 g, 9.79 mmol) as starting material, 3-amino-4-(cyclohexylamino)-N-(2-methoxyethyl)benzenesulfonamide **26** (2.13 g, 6.51 mmol) was generated. (Yield: 66.5%)

^{1}H NMR (400 MHz, DMSO-d_6) δ 1.15 - 1.25 (m, 3H), 1.28 - 1.43 (m, 2H), 1.58 - 1.67 (m, 1H), 1.69 - 1.79 (m, 2H), 1.91 - 2.02 (m, 2H), 2.81 (q, J = 6.1 Hz, 2H), 3.19 (s, 3H), 3.26 - 3.33 (m, 3H), 4.82 (d, J = 7.5 Hz, 1H), 4.92 (s, 2H), 6.50 (d, J = 8.9 Hz, 1H), 6.92 (s, 1H), 6.94 (d, J = 2.2 Hz, 1H), 7.03 (t, J = 6.1 Hz, 1H).

^{13}C NMR (101 MHz, DMSO-d_6) δ 25.14, 26.05, 33.04, 42.53, 51.21, 58.36, 71.08, 108.44, 112.05, 117.71, 126.45, 134.94, 138.64.

t_R 1.58 min, MS (ESI) m/z 328 [M +H] (100%)

3-amino-4-(cyclohexylamino)-N-(2-(methylamino)ethyl)benzenesulfonamide hydrochloride (27)

By following **General Procedure E** using tert-butyl (2-((3-amino-4-(cyclohexylamino)phenyl)sulfonamido)ethyl)(methyl)carbamate **21** (0.1 g, 0.23 mmol) as starting material to afford the desired 3-amino-4-(cyclohexylamino)-N-(2-(methylamino)ethyl)benzenesulfonamide hydrochloride **27** (0.024 g, 0.067 mmol). (Yield: 28.6%) The reported NMR spectrum is that of the hydrochloric acid form of **27**.

^{1}H NMR (400 MHz, DMSO-d_6) δ 1.14 - 1.26 (m, 3H), 1.29 - 1.45 (m, 2H), 1.57 - 1.67 (m, 1H), 1.69 - 1.79 (m, 2H), 1.92 - 1.99 (m, 2H), 2.18 (s, 3H), 2.46 (t, J = 6.6 Hz, 2H), 2.72 (t, J = 6.6 Hz, 2H), 3.23 - 3.37 (m, 1H), 4.85 (d, J = 7.5 Hz, 1H), 4.95 (s, 2H), 6.47 - 6.53 (m, 1H), 6.90 - 6.95 (m, 2H).

^{13}C NMR (101 MHz, DMSO-d_6) δ 24.66, 25.55, 32.53, 35.53, 42.02, 50.40, 50.69, 107.89, 111.47, 117.17, 125.77, 134.42, 138.04.

t_R 1.26 min, MS (ESI) m/z 327 [M +H] (100%)

3-amino-N-(2-aminoethyl)-4-(cyclohexylamino)benzenesulfonamide hydrochloride (28)

By following **General Procedure E** using tert-butyl (2-((3-amino-4-(cyclohexylamino)phenyl)sulfonamido)ethyl)carbamate **22** (0.15 g, 0.36 mmol) as starting material to afford the desired 3-amino-N-(2-aminoethyl)-4-(cyclohexylamino)benzenesulfonamide hydrochloride **28** (0.046 g, 0.132 mmol). (Yield: 36.3%) The reported NMR spectrum is that of the free base of **28**.

^{1}H NMR (400 MHz, DMSO-d_6) δ 1.10 - 1.44 (m, 7H), 1.58 - 1.69 (m, 1H), 1.69 - 1.79 (m, 2H), 1.93 - 2.00 (m, 2H), 2.51 - 2.55 (m, 2H), 2.66 (t, J = 6.3 Hz, 2H), 4.85 (d, J = 7.4 Hz, 1H), 4.95 (s, 2H), 6.50 (d, J = 9.0 Hz, 1H), 6.88 - 6.97 (m, 2H).

^{13}C NMR (101 MHz, DMSO-d_6) δ 24.67, 25.55, 32.54, 41.13, 45.87, 50.68, 107.87, 111.46, 117.16, 125.88, 134.40, 138.02.

t_R 1.17 min, MS (ESI) m/z 313 [M +H] (100%)

3-amino-4-(cyclohexylamino)-N-(2-(piperazin-1-yl)ethyl)benzenesulfonamide (29)

By following **General Procedure E** using tert-butyl 4-(2-((3-amino-4-(cyclohexylamino)phenyl)sulfonamido)ethyl)piperazine-1-carboxylate **23** (0.15 g, 0.36 mmol) as starting material to afford the desired 3-amino-4-(cyclohexylamino)-N-(2-(piperazin-1-

yl)ethyl)benzenesulfonamide **29** (0.120 g, 0.289 mmol). (Yield: 69.1%) The reported NMR spectrum is that of the free base of **29**.

^{1}H NMR (400 MHz, DMSO-d_6) δ 1.14 - 1.26 (m, 4H), 1.29 - 1.43 (m, 2H), 1.58 - 1.68 (m, 1H), 1.68 - 1.78 (m, 2H), 1.91 - 2.03 (m, 2H), 2.13 - 2.21 (m, 4H), 2.22 - 2.29 (m, 2H), 2.62 (t, J = 4.9 Hz, 4H), 2.74 (t, J = 7.1 Hz, 2H), 3.26 - 3.30 (m, 1H), 4.86 (d, J = 7.5 Hz, 1H), 4.96 (s, 2H), 6.50 (d, J = 9.0 Hz, 1H), 6.74 - 6.84 (m, 1H), 6.87 - 6.96 (m, 2H).

^{13}C NMR (101 MHz, DMSO-d_6) δ 24.66, 25.55, 32.52, 45.38, 50.68, 53.96, 57.41, 107.89, 111.47, 117.20, 125.60, 134.45, 138.07.

t_R 1.17 min, MS (ESI) m/z 381 [M +H] (100%)

3-(benzylamino)-4-(cyclohexylamino)-N-(2-(dimethylamino)ethyl)benzenesulfonamide (30)

By following **General Procedure D,** the reaction mixture was prepared using 3-amino-4-(cyclohexylamino)-N-(2-(dimethylamino)ethyl)benzenesulfonamide **20** (0.300 g, 0.881 mmol, 1equiv.), bromomethylbenzene (0.105 mL, 0.881 mmol, 1 equiv.) and potassium carbonate (0.122 g, 0.881 mmol, 1 equiv.). This mixture was allowed to stir for 15 minutes at room temperature. The mixture was diluted with water and washed with EtOAc. The aqueous layer was concentrated, lyophilisated and purified further using reverse phase flash chromatography (Water/MeOH) to afford the desired 3-(benzylamino)-4-(cyclohexylamino)-N-(2-(dimethylamino)ethyl)benzenesulfonamide **30** (0.151 g, 0.351 mmol) (Yield: 40%)

^{1}H NMR (400 MHz, Acetone-d_6) δ 1.18 - 1.48 (m, 5H), 1.61 - 1.70 (m, 1H), 1.74 - 1.82 (m, 2H), 2.01 - 2.09 (m, 2H), 3.32 (s, 6H), 3.35 - 3.42 (m, 1H), 3.50 (t, J = 5.9 Hz, 2H), 3.79 (t, J = 6.0 Hz, 2H), 4.76 - 4.82 (m, 2H), 4.97 (s, 2H), 6.58 (d, J = 8.4 Hz, 1H), 7.18 (dd, J = 8.4, 2.2 Hz, 1H), 7.35 (d, J = 2.2 Hz, 1H), 7.47 - 7.57 (m, 3H), 7.75 - 7.78 (m, 2H).

^{13}C NMR (101 MHz, Acetone-d_6) δ 25.85, 26.66, 33.72, 38.36, 50.91, 52.23, 64.79, 68.57, 109.18, 114.01, 119.81, 126.66, 128.97, 129.83, 131.29, 134.32, 135.67, 140.63.

t_R 1.51 min, MS (ESI) m/z 431 [M +H] (100%)

tert-butyl (2-((3-(benzylamino)-4-(cyclohexylamino)phenyl)sulfonamido)ethyl)(methyl)carbamate (31)

By following **General Procedure D,** the reaction mixture was prepared using tert-butyl (2-((3-amino-4-(cyclohexylamino)phenyl)sulfonamido)ethyl)(methyl)carbamate **21** (0.100 g, 0.234 mmol, 1 equiv.), bromomethylbenzene (0.028 mL, 0.234 mmol, 1 equiv.) and potassium carbonate (0.032 g, 0.234 mmol, 1 equiv.). This mixture was allowed to stir for 45 minutes at 40°C. The mixture was diluted with water and washed with EtOAc. The organic layer was concentrated to afford tert-butyl (2-((3-(benzylamino)-4-(cyclohexylamino)phenyl)sulfonamido)ethyl)(methyl)carbamate **31** which was introduced in the next step without further purification.

tert-butyl (2-((3-(benzylamino)-4-(cyclohexylamino)phenyl)sulfonamido)ethyl)carbamate (32)

By following **General Procedure D,** the reaction mixture was prepared using tert-butyl (2-((3-amino-4-(cyclohexylamino)phenyl)sulfonamido)ethyl)carbamate **22** (0.200 g, 0.485 mmol, 1equiv.), bromomethylbenzene (0.058 mL, 0.485 mmol, 1 equiv.) and potassium carbonate (0.080 g, 0.485 mmol, 1 equiv.). This mixture was allowed to stir for 60 minutes at 40°C. The mixture was diluted with water and washed with EtOAc. The organic layer was concentrated to afford tert-butyl (2-((3-(benzylamino)-4-(cyclohexylamino)phenyl)sulfonamido)ethyl)carbamate **32** which was introduced in the next step without further purification.

tert-butyl 4-(2-((3-(benzylamino)-4-(cyclohexylamino)phenyl)sulfonamido)ethyl)piperazine-1-carboxylate (33)

By following **General Procedure D,** the reaction mixture was prepared using tert-butyl 4-(2-((3-amino-4-(cyclohexylamino)phenyl)sulfonamido)ethyl)piperazine-1-carboxylate **23** (0.300 g, 0.623 mmol, 1equiv.), bromomethylbenzene (0.074 mL, 0.623 mmol, 1 equiv.) and potassium carbonate (0.172 g, 0.623 mmol, 1 equiv.). This mixture was allowed to stir for 60 minutes at 40°C. The mixture was diluted with water and washed with EtOAc. The aqueous layer was concentrated and purified further using normal phase flash chromatography (Heptane/Ethyl acetate) to afford the desired tert-butyl 4-(2-((3-(benzylamino)-4-(cyclohexylamino)phenyl)sulfonamido)ethyl)piperazine-1-carboxylate **33** (0.135 g, 0.236 mmol) (Yield: 37.9%)

^{1}H NMR (400 MHz, DMSO-d_6) δ 1.14 - 1.30 (m, 3H), 1.32 - 1.38 (m, 2H), 1.39 (s, 9H), 1.60 - 1.69 (m, 1H), 1.70 - 1.80 (m, 2H), 1.94 - 2.05 (m, 2H), 2.10 - 2.19 (m, 4H), 2.21 (t, J = 6.8 Hz, 2H), 2.55 - 2.64 (m, 2H), 3.17 - 3.28 (m, 4H), 3.29 - 3.35 (m, 1H), 4.32 (d, J = 5.4 Hz, 2H), 5.13 (d, J = 7.2 Hz, 1H), 5.69 (t, J = 5.6 Hz, 1H), 6.55 (d, J = 8.5 Hz, 1H), 6.73 (d, J = 2.1 Hz, 1H), 6.78 (t, J = 5.8 Hz, 1H), 6.98 (dd, J = 8.3, 2.1 Hz, 1H), 7.21 - 7.41 (m, 5H).

^{13}C NMR (101 MHz, DMSO-d_6) δ 24.67, 25.57, 28.01, 32.46, 42.67, 43.67, 46.89, 50.85, 52.20, 56.43, 78.66, 107.49, 117.22, 125.80, 126.77, 127.33, 128.28, 134.49, 138.33, 139.42, 153.70.

3-(benzylamino)-4-(cyclohexylamino)-N-(2-(4-methylpiperazin-1-yl)ethyl)benzenesulfonamide (34)

By following **General Procedure D,** the reaction mixture was prepared using 3-amino-4-(cyclohexylamino)-N-(2-(4-methylpiperazin-1-yl)ethyl)benzenesulfonamide **24** (0.200 g, 0.506 mmol, 1equiv.), bromomethylbenzene (0.060 mL, 0.506 mmol, 1 equiv.) and potassium carbonate (0.070 g, 0.506 mmol, 1 equiv.). This mixture was allowed to stir for 10 minutes at room temperature. The mixture was diluted with water and washed with EtOAc. The aqueous layer was concentrated, lyophilisated and purified further using reverse phase flash chromatography (Water/MeOH) to afford the desired 3-(benzylamino)-4-(cyclohexylamino)-N-(2-(4-methylpiperazin-1-yl)ethyl)benzenesulfonamide **34** (0.066 g, 0.136 mmol) (Yield: 26.9%)

^{1}H NMR (400 MHz, Methanol-d_4) δ 1.21 - 1.35 (m, 3H), 1.36 - 1.52 (m, 2H), 1.66 - 1.75 (m, 1H), 1.81 (dt, J = 13.3, 3.4 Hz, 2H), 2.00 - 2.12 (m, 2H), 2.53 (dd, J = 6.6, 5.2 Hz, 2H), 2.62 (ddd, J = 13.2, 9.7, 2.7 Hz, 2H), 2.78 (dt, J = 13.5, 3.7 Hz, 2H), 2.94 - 3.06 (m, 5H), 3.26 - 3.30 (m, 2H), 3.35 - 3.41 (m, 1H), 3.43 - 3.56 (m, 2H), 4.62 (s, 2H), 6.63 (d, J = 8.4 Hz, 1H), 7.18 - 7.25 (m, 2H), 7.50 - 7.64 (m, 5H).

^{13}C NMR (101 MHz, Methanol-d_4) δ 26.28, 27.05, 34.10, 41.03, 47.05, 52.70, 56.40, 61.04, 69.95, 109.77, 114.53, 120.83, 127.11, 128.24, 130.36, 131.95, 134.46, 135.33, 141.30.

t_R 1.48 min, MS (ESI) m/z 486 [M +H] (100%)

3-(benzylamino)-4-(cyclohexylamino)-N-(2-morpholinoethyl)benzenesulfonamide (35)

By following **General Procedure D,** the reaction mixture was prepared using 3-amino-4-(cyclohexylamino)-N-(2-morpholinoethyl)benzenesulfonamide **25** (0.300 g, 0.784 mmol, 1equiv.), bromomethylbenzene (0.094 mL, 0.784 mmol, 1 equiv.) and potassium carbonate (0.108 g, 0.784 mmol, 1 equiv.). This mixture was allowed to stir for 20 minutes at 40°C. The mixture was diluted with water and washed with EtOAc. The aqueous layer was concentrated, lyophilisated and purified further using reverse phase flash chromatography (Water/MeOH) to afford the desired 3-(benzylamino)-4-(cyclohexylamino)-N-(2-morpholinoethyl)benzenesulfonamide **35**. (0.065 g, 0.138 mmol.) (Yield: 17.5%)

^{1}H NMR (400 MHz, Acetone-d_6) δ 1.21 - 1.33 (m, 3H), 1.38 - 1.51 (m, 2H), 1.64 - 1.70 (m, 1H), 1.74 - 1.83 (m, 2H), 2.05 - 2.13 (m, 2H), 2.16 - 2.20 (m, 4H), 2.28 (t, J = 6.6, 5.8 Hz, 2H), 2.76 (q, J = 6.4, 5.7 Hz, 2H), 3.39 - 3.49 (m, 1H), 3.52 (t, 4H), 4.40 (d, J = 5.4 Hz, 2H), 4.65 (d, J = 7.2 Hz, 1H), 4.84 (t, J = 5.5 Hz, 1H), 5.57 (t, J = 5.6 Hz, 1H), 6.71 (d, J = 8.4 Hz, 1H), 7.01 (d, J = 2.1 Hz, 1H), 7.18 (dd, J = 8.3, 2.1 Hz, 1H), 7.24 - 7.30 (m, 1H), 7.32 - 7.38 (m, 2H), 7.40 - 7.44 (m, 2H).

^{13}C NMR (101 MHz, Acetone-d_6) δ 25.76, 26.68, 33.74, 40.37, 48.73, 52.26, 54.01, 57.47, 67.31, 109.35, 110.47, 119.54, 127.76, 127.89, 128.55, 129.31, 136.11, 140.37, 140.61.

t_R 1.66 min, MS (ESI) m/z 473 [M +H] (100%)

3-(benzylamino)-4-(cyclohexylamino)-N-(2-methoxyethyl)benzenesulfonamide (36)

By following **General Procedure D,** the reaction mixture was prepared using 3-amino-4-(cyclohexylamino)-N-(2-methoxyethyl)benzenesulfonamide **26** (0.300 g, 0.916 mmol, 1 equiv.), bromomethylbenzene (0.110 mL, 0.916 mmol, 1 equiv.) and potassium carbonate (0.127 g, 0.916 mmol, 1 equiv.). This mixture was allowed to stir for 4 hours at 60°C. The mixture was diluted with EtOAc and washed with water. The organic layer was dried using anhydrous sodium sulfate, concentrated and purified further using preperative HPLC (Water/Acetonitrile) to afford the desired 3-(benzylamino)-4-(cyclohexylamino)-N-(2-methoxyethyl)benzenesulfonamide **36** (0.020 g, 0.048 mmol) (Yield: 5.23%)

^{1}H NMR (400 MHz, Methanol-*d*$_4$) δ 1.22 - 1.36 (m, 3H), 1.36 - 1.53 (m, 2H), 1.66 - 1.77 (m, 1H), 1.83 (dt, J = 13.1, 3.7 Hz, 2H), 2.11 (dd, J = 13.3, 3.4 Hz, 2H), 2.72 (t, J = 5.6 Hz, 2H), 3.23 (d, J = 3.5 Hz, 5H), 3.37 - 3.42 (m, 1H), 4.40 (s, 2H), 6.62 - 6.67 (m, 1H), 6.89 (d, J = 2.1 Hz, 1H), 7.15 (dd, J = 8.4, 2.1 Hz, 1H), 7.21 - 7.27 (m, 1H), 7.32 (ddd, J = 7.6, 6.8, 1.2 Hz, 2H), 7.39 (ddt, J = 7.7, 1.5, 0.7 Hz, 2H).
^{13}C NMR (101 MHz, Methanol-*d*$_4$) δ 26.29, 27.10, 34.11, 43.57, 48.89, 52.82, 58.84, 72.03, 109.62, 110.66, 119.71, 127.10, 128.04, 128.60, 129.54, 136.35, 140.80, 141.25.

t_R 2.18 min, MS (ESI) m/z 418 [M +H] (100%)

3-(benzylamino)-4-(cyclohexylamino)-N-(2-(methylamino)ethyl)benzenesulfonamide hydrochloride (37)

By following **General Procedure E** using tert-butyl (2-((3-(benzylamino)-4-(cyclohexylamino)phenyl)sulfonamido)ethyl)(methyl)carbamate **31** (0.300 g, 0.581mmol) as starting material to afford the desired 3-(benzylamino)-4-(cyclohexylamino)-N-(2-(methylamino)ethyl)benzenesulfonamide hydrochloride **37** (0.075 g, 0.166 mmol). (Yield: 28.5%) The reported NMR spectrum is that of the free base of **37**.

^{1}H NMR (400 MHz, DMSO-d_6) δ 1.14 - 1.29 (m, 3H), 1.30 - 1.44 (m, 2H), 1.59 - 1.69 (m, 1H), 1.70 - 1.82 (m, 2H), 1.95 - 2.03 (m, 2H), 2.15 (s, 3H), 2.37 (t, J = 6.4 Hz, 2H), 2.55 (t, J = 6.4 Hz, 2H), 3.30 - 3.42 (m, 1H), 4.32 (d, J = 5.3 Hz, 2H), 5.14 (d, J = 7.2 Hz, 1H), 5.69 (t, J = 5.6 Hz, 1H), 6.54 (d, J = 8.4 Hz, 1H), 6.72 (d, J = 2.1 Hz, 1H), 6.96 (dd, J = 8.3, 2.1 Hz, 1H), 7.20 - 7.43 (m, 5H).

^{13}C NMR (101 MHz, DMSO-d_6) δ 24.68, 25.57, 32.47, 35.50, 41.90, 46.91, 50.30, 50.85, 107.43, 117.16, 125.92, 126.78, 127.37, 128.29, 134.50, 138.32, 139.40.

t_R 1.82 min, MS (ESI) m/z 417 [M +H] (100%)

N-(2-aminoethyl)-3-(benzylamino)-4-(cyclohexylamino)benzenesulfonamide hydrochloride (38)

By following **General Procedure E** using tert-butyl (2-((3-(benzylamino)-4-(cyclohexylamino)phenyl)sulfonamido)ethyl)carbamate **32** (0.150 g, 0.298mmol) as starting material to afford the desired N-(2-aminoethyl)-3-(benzylamino)-4-(cyclohexylamino)benzenesulfonamide hydrochloride **38** (0.034 g, 0.078 mmol). (Yield: 26.1%) The reported NMR spectrum is that of the hydrochloric salt of **38**.

^{1}H NMR (400 MHz, DMSO-d_6) δ 1.12 - 1.29 (m, 3H), 1.31 - 1.45 (m, 2H), 1.64 (m, 1H), 1.70 - 1.82 (m, 2H), 1.94 - 2.06 (m, 2H), 2.38 - 2.45 (m, 2H), 2.45 - 2.49 (m, 2H), 3.25 - 3.41 (m, 1H), 4.32 (d, J = 5.3 Hz, 2H), 5.13 (d, J = 7.2 Hz, 1H), 5.68 (t, J = 5.6 Hz, 1H), 6.54 (d, J = 8.4 Hz, 1H), 6.71 (d, J = 2.1 Hz, 1H), 6.96 (dd, J = 8.4, 2.1 Hz, 1H), 7.20 - 7.30 (m, 1H), 7.30 - 7.42 (m, 4H).

^{13}C NMR (101 MHz, DMSO-d_6) δ 24.69, 25.57, 32.49, 41.16, 46.07, 46.92, 50.86, 107.43, 117.14, 126.08, 126.78, 127.38, 128.30, 134.48, 138.29, 139.39.

t_R 1.81 min, MS (ESI) 403 m/z [M +H] (100%)

3-(benzylamino)-4-(cyclohexylamino)-N-(2-(piperazin-1-yl)ethyl)benzenesulfonamide hydrochloride (39)

By following **General Procedure E** using tert-butyl 4-(2-((3-(benzylamino)-4-(cyclohexylamino)phenyl)sulfonamido)ethyl)piperazine-1-carboxylate **33** (0.135 g, 0.245 mmol) as starting material to afford the desired 3-(benzylamino)-4-(cyclohexylamino)-N-(2-(piperazin-1-yl)ethyl)benzenesulfonamide hydrochloride **39** (0.110 g, 0.216 mmol). (Yield: 88%). The reported NMR spectrum is that of the free base of **39**.

^{1}H NMR (400 MHz, DMSO-d_6) δ 1.15 - 1.29 (m, 4H), 1.31 - 1.45 (m, 2H), 1.59 - 1.68 (m, 1H), 1.70 - 1.80 (m, 2H), 1.95 - 2.04 (m, 2H), 2.10 - 2.21 (m, 6H), 2.56 (t, J = 7.1 Hz, 2H), 2.61 (t, J = 4.8 Hz, 4H), 3.33 - 3.39 (m, 1H), 4.32 (d, J = 5.3 Hz, 2H), 5.13 (d, J = 7.2 Hz, 1H), 5.69 (t, J = 5.7 Hz, 1H), 6.54 (d, J = 8.4 Hz, 1H), 6.72 (d, J = 2.1 Hz, 1H), 6.74 - 6.80 (m, 1H), 6.97 (dd, J = 8.3, 2.1 Hz, 1H), 7.20 - 7.29 (m, 1H), 7.30 - 7.40 (m, 4H).

^{13}C NMR (101 MHz, DMSO-d_6) δ 24.68, 25.57, 32.46, 39.73, 45.38, 46.88, 50.86, 53.89, 57.34, 107.48, 117.20, 125.76, 126.76, 127.33, 128.28, 134.49, 138.33, 139.40.

t_R 1.44 min, MS (ESI) m/z 472 [M +H] 100(%)

4-(cyclohexylamino)-N-(2-(dimethylamino)ethyl)-3-((pyridin-4-ylmethyl)amino)benzenesulfonamide (40)

By following **General Procedure D,** the reaction mixture was prepared using 3-amino-4-(cyclohexylamino)-N-(2-(dimethylamino)ethyl)benzenesulfonamide **20** (0.293 g, 0.861 mmol, 1equiv.), 4-(bromomethyl)pyridine hydrobromide (0.218 g, 0.861 mmol, 1 equiv.) and potassium carbonate (0.119 g, 0.861 mmol, 1 equiv.). This mixture was allowed to stir for 30 minutes at room temperature. The mixture was diluted with water and washed with EtOAc. The aqueous layer was concentrated, lyophilisated and purified further using reverse phase flash chromatography (Water/MeOH) to afford the desired 4-

(cyclohexylamino)-N-(2-(dimethylamino)ethyl)-3-((pyridin-4-ylmethyl)amino)benzenesulfonamide **40** (0.170 g, 0.394 mmol) (Yield: 45.8 %)

^{1}H NMR (400 MHz, Methanol-*d*$_4$) δ 1.23 - 1.35 (m, 3H), 1.37 - 1.50 (m, 2H), 1.70 (dt, J = 12.8, 3.6 Hz, 1H), 1.81 (dt, J = 13.3, 3.6 Hz, 2H), 2.02 - 2.10 (m, 2H), 3.19 (s, 6H), 3.34 - 3.39 (m, 1H), 3.43 (t, J = 6.2 Hz, 2H), 3.59 (t, J = 6.3 Hz, 2H), 4.72 (s, 2H), 6.63 (d, J = 9.1 Hz, 1H), 7.21 - 7.25 (m, 2H), 7.63 - 7.66 (m, 2H), 8.68 - 8.71 (m, 2H).

^{13}C NMR (101 MHz, Methanol-*d*$_4$) δ 26.30, 27.05, 34.08, 38.44, 51.70, 52.69, 64.96, 67.94, 109.97, 114.39, 121.01, 125.56, 129.35, 135.46, 138.05, 141.76, 151.35.

t_R 1.35 min, MS (ESI) m/z 432 [M +H] (100%)

tert-butyl (2-((4-(cyclohexylamino)-3-((pyridin-4-ylmethyl)amino)phenyl)sulfonamido)ethyl)(methyl)carbamate (41)

By following **General Procedure D,** the reaction mixture was prepared using tert-butyl (2-((3-amino-4-(cyclohexylamino)phenyl)sulfonamido)ethyl)(methyl)carbamat**e 21** (0.250 g, 0.586 mmol, 1 equiv.), 4-(bromomethyl)pyridine hydrobromide (0.148 g, 0.586 mmol, 1 equiv.) and potassium carbonate (0.081 g, 0.586 mmol, 1 equiv.). This mixture was allowed to stir for 40 minutes at 40°C. The mixture was diluted with water and washed with EtOAc. The aqueous layer was concentrated and purified further using normal phase flash chromatography (Heptane/Ethyl acetate) to afford the desired tert-butyl (2-((4-(cyclohexylamino)-3-((pyridin-4-ylmethyl)amino)phenyl)sulfonamido)ethyl)(methyl)carbamate **41** (0.070 g, 0.135 mmol) (Yield: 23.1 %). The compound was immediately introduced in the next step.

tert-butyl (2-((4-(cyclohexylamino)-3-((pyridin-4-ylmethyl)amino)phenyl)sulfonamido)ethyl)carbamate (42)

By following **General Procedure D,** the reaction mixture was prepared using tert-butyl (2-((3-amino-4-(cyclohexylamino)phenyl)sulfonamido)ethyl)carbamate **22** (0.400 g, 0.970 mmol, 1 equiv.), 4-(bromomethyl)pyridine hydrobromide (0.490 g, 1.939 mmol, 2 equiv.) and potassium carbonate (0.402 g, 2.91 mmol, 3 equiv.). This mixture was allowed to stir for 60 minutes at 40°C. The mixture was diluted with water and washed with EtOAc. The aqueous layer was concentrated and purified further using normal phase flash chromatography (Heptane/Ethyl acetate) to afford the desired tert-butyl (2-((4-(cyclohexylamino)-3-((pyridin-4-ylmethyl)amino)phenyl)sulfonamido)ethyl)carbamate **42** (0.200 g, 0.387 mmol) (Yield: 41.0 %).

^{1}H NMR (400 MHz, Acetone-d_6) δ 1.27 - 1.36 (m, 3H), 1.40 (s, 9H), 1.43 - 1.51 (m, 2H), 1.63 - 1.72 (m, 1H), 1.74 - 1.83 (m, 2H), 2.12 (d, J = 3.9 Hz, 2H), 2.79 (q, J = 6.3 Hz, 2H), 3.08 (q, J = 6.2 Hz, 2H), 3.38 - 3.51 (m, 1H), 4.46 (d, J = 5.4 Hz, 2H), 4.57 - 4.66 (m, 1H), 4.93 - 5.06 (m, 1H), 5.92 (s, 1H), 6.03 - 6.12 (m, 1H), 6.72 (d, J = 8.4 Hz, 1H), 6.92 (d, J = 2.1 Hz, 1H), 7.20 (dd, J = 8.3, 2.1 Hz, 1H), 7.38 (dd, J = 4.7, 1.6 Hz, 2H), 8.47 - 8.59 (m, 2H).

^{13}C NMR (101 MHz, Acetone-d_6) δ 24.79, 25.76, 27.73, 32.88, 43.09, 46.67, 51.38, 78.00, 108.73, 109.76, 119.09, 122.44, 127.37, 134.81, 139.94, 148.69, 149.78, 155.96.

tert-butyl 4-(2-((4-(cyclohexylamino)-3-((pyridin-4-ylmethyl)amino)phenyl)sulfonamido)ethyl)piperazine-1-carboxylate (43)

By following **General Procedure D,** the reaction mixture was prepared using tert-butyl 4-(2-((3-amino-4-(cyclohexylamino)phenyl)sulfonamido)ethyl)piperazine-1-carboxylate **23** (0.400 g, 0.830 mmol, 1 equiv.), 4-(bromomethyl)pyridine hydrobromide (0.420 g, 1.661 mmol, 2 equiv.) and potassium carbonate (0.344 g, 2.491 mmol, 3 equiv.). This mixture was allowed to stir for 2 hours at 40°C. The mixture was diluted with water and washed with EtOAc. The aqueous layer was concentrated and purified further using normal phase flash chromatography (Heptane/Ethyl acetate) to afford the desired tert-butyl 4-(2-((4-

(cyclohexylamino)-3-((pyridin-4-ylmethyl)amino)phenyl)sulfonamido)ethyl)piperazine-1-carboxylate **43** (0.160 g, 0.279 mmol) (Yield: 33.6 %).

^{1}H NMR (400 MHz, DMSO-*d_6*) δ 1.24 (s, 3H), 1.39 (s, 11H), 1.62 - 1.69 (m, 1H), 1.72 - 1.79 (m, 2H), 1.97 - 2.06 (m, 2H), 2.13 (t, J = 5.0 Hz, 4H), 2.18 (t, J = 6.8 Hz, 2H), 2.53 - 2.59 (m, 2H), 3.18 - 3.28 (m, 4H), 3.38 (s, 1H), 4.38 (d, J = 5.5 Hz, 2H), 5.10 (d, J = 7.2 Hz, 1H), 5.82 (t, J = 5.7 Hz, 1H), 6.57 (d, J = 8.5 Hz, 1H), 6.61 (d, J = 2.1 Hz, 1H), 6.78 (t, J = 5.8 Hz, 1H), 6.98 (dd, J = 8.3, 2.1 Hz, 1H), 7.30 - 7.37 (m, 2H), 8.47 - 8.55 (m, 2H).

^{13}C NMR (101 MHz, Acetone-*d_6*) δ 25.73, 26.69, 28.62, 33.76, 40.60, 44.38, 47.46, 52.28, 53.29, 57.03, 79.53, 109.68, 110.56, 119.88, 123.32, 127.91, 135.61, 140.74, 149.65, 150.68, 154.97.

4-(cyclohexylamino)-N-(2-(4-methylpiperazin-1-yl)ethyl)-3-((pyridin-4-ylmethyl)amino)benzenesulfonamide (44)

By following **General Procedure D,** the reaction mixture was prepared using 3-amino-4-(cyclohexylamino)-N-(2-(4-methylpiperazin-1-yl)ethyl)benzenesulfonamide **24** (0.300 g, 0.758 mmol, 1equiv.), 4-(bromomethyl)pyridine hydrobromide (0.0.192 g, 0.758 mmol, 1 equiv.) and potassium carbonate (0.105 g, 0.758 mmol, 1 equiv.). This mixture was allowed to stir for 15 minutes at room temperature. The mixture was diluted with water and washed with EtOAc. The aqueous layer was concentrated, lyophilisated and purified further using reverse phase flash chromatography (Water/MeOH) to afford the desired 4-(cyclohexylamino)-N-(2-(4-methylpiperazin-1-yl)ethyl)-3-((pyridin-4-ylmethyl)amino)benzenesulfonamide **44** (0.170 g, 0.349 mmol) (Yield: 46.1 %)

^{1}H NMR (400 MHz, Methanol-*d_4*) δ 1.22 - 1.34 (m, 3H), 1.36 - 1.50 (m, 2H), 1.69 (dt, J = 12.8, 3.8 Hz, 1H), 1.80 (dt, J = 13.2, 3.7 Hz, 2H), 1.99 - 2.10 (m, 2H), 2.52 (t, J = 6.0 Hz, 2H), 2.58 - 2.67 (m, 2H), 2.71 - 2.79 (m, 2H), 3.00 (t, J = 6.0 Hz, 2H), 3.05 (s, 3H), 3.34 - 3.40 (m, 3H), 3.55 - 3.64 (m, 2H), 4.74 (s, 2H), 6.63 (d, J = 8.5 Hz, 1H), 7.21 (dd, J = 8.4, 2.3 Hz, 1H), 7.29 (d, J = 2.2 Hz, 1H), 7.69 - 7.71 (m, 2H), 8.70 - 8.73 (m, 2H).

^{13}C NMR (101 MHz, Methanol-d_4) δ 26.32, 27.06, 34.12, 41.03, 46.96, 52.71, 56.22, 61.67, 109.75, 114.37, 120.85, 127.09, 129.54, 135.48, 137.79, 141.25, 151.31.

t_R 1.35 min, MS (ESI) m/z 487 [M +H] (100%)

4-(cyclohexylamino)-N-(2-morpholinoethyl)-3-((pyridin-4-ylmethyl)amino)benzenesulfonamide (45)

By following **General Procedure D,** the reaction mixture was prepared using 3-amino-4-(cyclohexylamino)-N-(2-morpholinoethyl)benzenesulfonamide **25** (0.200 g, 0.523 mmol, 1equiv.), 4-(bromomethyl)pyridine hydrobromide (0.246 g, 1.046 mmol, 2 equiv.) and potassium carbonate (0.217 g, 1.569 mmol, 3 equiv.). This mixture was allowed to stir for 2 hours at 60°C. The mixture was diluted with EtOAc and washed with water. The organic layer was dried using anhydrous sodium sulfate, concentrated and purified further using normal phase flash chromatography on silica gel (Heptanes/EtOAc/MeOH) to afford the desired 4-(cyclohexylamino)-N-(2-morpholinoethyl)-3-((pyridin-4-ylmethyl)amino)benzenesulfonamide **45** (0.065 g, 0.137 mmol) (Yield: 26.3 %)

^{1}H NMR (400 MHz, Methanol-d_4) δ 1.24 - 1.36 (m, 3H), 1.39 - 1.52 (m, 2H), 1.71 (dt, J = 13.1, 3.6 Hz, 1H), 1.82 (dt, J = 13.2, 3.7 Hz, 2H), 2.06 - 2.14 (m, 2H), 2.25 - 2.30 (m, 6H), 2.73 (t, J = 6.5 Hz, 2H), 3.39 (tt, J = 10.4, 3.7 Hz, 1H), 3.59 (t, J = 4.7 Hz, 4H), 4.46 (s, 2H), 6.66 (d, J = 8.5 Hz, 1H), 6.78 (d, J = 2.1 Hz, 1H), 7.19 (dd, J = 8.4, 2.1 Hz, 1H), 7.41 - 7.44 (m, 2H), 8.43 - 8.46 (m, 2H).

^{13}C NMR (101 MHz, Methanol-d_4) δ 26.28, 27.11, 34.13, 40.59, 47.50, 52.81, 54.44, 58.28, 67.60, 109.80, 110.24, 120.25, 124.15, 126.87, 135.74, 141.26, 150.13, 152.08.

t_R 1.34 min, MS (ESI) m/z 474 [M +H] (100%)

4-(cyclohexylamino)-N-(2-methoxyethyl)-3-((pyridin-4-ylmethyl)amino)benzenesulfonamide (46)

By following **General Procedure D,** the reaction mixture was prepared using 3-amino-4-(cyclohexylamino)-N-(2-methoxyethyl)benzenesulfonamide **26** (0.400 g, 1.222 mmol, 1 equiv.), 4-(bromomethyl)pyridine hydrobromide (0.618 g, 2.443 mmol, 2 equiv.) and potassium carbonate (0.506 g, 3.66 mmol, 3 equiv.). This mixture was allowed to stir for 4 hours at 60°C. The mixture was diluted with EtOAc and washed with water. The organic layer was dried using anhydrous sodium sulfate, concentrated and purified further using normal phase flash chromatography on silica gel (Heptanes/EtOAc) to afford the desired 4-(cyclohexylamino)-N-(2-methoxyethyl)-3-((pyridin-4-ylmethyl)amino)benzenesulfonamide **46** (0.212 g, 0.507 mmol) (Yield: 41.5 %)

^{1}H NMR (400 MHz, DMSO-*d*$_6$) δ 1.18 - 1.36 (m, 3H), 1.36 - 1.51 (m, 2H), 1.63 - 1.73 (m, 1H), 1.73 - 1.85 (m, 2H), 1.98 - 2.10 (m, 2H), 2.64 (q, J = 6.0 Hz, 2H), 3.19 (s, 3H), 3.22 (t, J = 6.0 Hz, 2H), 3.39 (ddt, J = 8.9, 6.0, 3.1 Hz, 1H), 4.45 (s, 2H), 5.14 (s, 1H), 5.89 (s, 1H), 6.61 (d, J = 8.4 Hz, 1H), 6.65 (d, J = 2.1 Hz, 1H), 7.00 - 7.09 (m, 2H), 7.40 - 7.50 (m, 2H), 8.50 - 8.66 (m, 2H).

^{13}C NMR (101 MHz, DMSO-*d*$_6$) δ 25.11, 26.05, 32.97, 42.41, 46.25, 51.38, 58.30, 70.96, 108.15, 108.28, 118.08, 123.09, 126.62, 134.50, 139.04, 149.18, 150.64.

t_R 1.37 min, MS (ESI) m/z 419 [M +H] (100%)

4-(cyclohexylamino)-N-(2-(methylamino)ethyl)-3-((pyridin-4-ylmethyl)amino)benzenesulfonamide hydrochloride (47)

By following **General Procedure E** using tert-butyl (2-((4-(cyclohexylamino)-3-((pyridin-4-ylmethyl)amino)phenyl)sulfonamido)ethyl)(methyl)carbamate **41** (0.070 g, 0.135 mmol) as starting material to afford the desired 4-(cyclohexylamino)-N-(2-(methylamino)ethyl)-3-((pyridin-4-ylmethyl)amino)benzenesulfonamide hydrochloride **47** (0.059 g, 0.130 mmol). (Yield: 96%).The reported NMR spectrum is that of the free base of **47**.

^{1}H NMR (400 MHz, DMSO-d_6) δ 1.21 - 1.35 (m, 3H), 1.38 - 1.51 (m, 2H), 1.65 - 1.74 (m, 1H), 1.77 - 1.86 (m, 2H), 2.01 - 2.10 (m, 2H), 2.19 (s, 3H), 2.39 (t, J = 6.4 Hz, 2H), 2.54 - 2.56 (m, 2H), 3.35 - 3.46 (m, 1H), 4.43 (d, J = 5.4 Hz, 2H), 5.18 (d, J = 7.1 Hz, 1H), 5.90 (t, J = 5.6 Hz, 1H), 6.62 (d, J = 8.5 Hz, 1H), 6.65 (d, J = 2.1 Hz, 1H), 7.03 (dd, J = 8.4, 2.1 Hz, 1H), 7.29 - 7.48 (m, 2H), 8.49 - 8.63 (m, 2H).

^{13}C NMR (101 MHz, DMSO-d_6) δ 24.64, 25.56, 32.46, 35.50, 41.86, 45.70, 50.26, 50.84, 107.50, 107.68, 117.48, 122.29, 125.96, 134.04, 138.42, 148.82, 149.52.

t_R 1.19 min, MS (ESI) m/z 418 [M +H] (100%)

N-(2-aminoethyl)-4-(cyclohexylamino)-3-((pyridin-4-ylmethyl)amino)benzenesulfonamide hydrochloride (48)

By following **General Procedure E** using tert-butyl (2-((4-(cyclohexylamino)-3-((pyridin-4-ylmethyl)amino)phenyl)sulfonamido)ethyl)carbamate **42** (0.050 g, 0.124 mmol) as starting material to afford the desired 4 N-(2-aminoethyl)-4-(cyclohexylamino)-3-((pyridin-4-ylmethyl)amino)benzenesulfonamide hydrochloride **48** (0.039 g, 0.089 mmol). (Yield: 71.1%).The reported NMR spectrum is that of the free base of **48**.

^{1}H NMR (400 MHz, Methanol-d_4) δ 1.22 - 1.39 (m, 3H), 1.40 - 1.54 (m, 2H), 1.68 - 1.79 (m, 1H), 1.80 - 1.88 (m, 2H), 2.06 - 2.16 (m, 2H), 2.84 (t, J = 6.7 Hz, 2H), 3.16 (t, J = 6.7 Hz, 2H), 3.35 - 3.46 (m, 1H), 4.48 (s, 2H), 6.67 (d, J = 8.4 Hz, 1H), 6.77 (d, J = 2.1 Hz, 1H), 7.18 (dd, J = 8.4, 2.1 Hz, 1H), 7.35 - 7.55 (m, 2H), 8.29 - 8.51 (m, 2H).

^{13}C NMR (101 MHz, Methanol-d_4) δ 26.26, 27.10, 34.13, 44.24, 47.52, 51.57, 52.80, 109.76, 110.22, 120.20, 124.10, 127.31, 135.77, 141.24, 150.09, 150.11, 152.10.

t_R 1.24 min, MS (ESI) m/z 404 [M +H] (100%)

4-(cyclohexylamino)-N-(2-(piperazin-1-yl)ethyl)-3-((pyridin-4-ylmethyl)amino)benzenesulfonamide hydrochloride (49)

By following **General Procedure E** using tert-butyl 4-(2-((4-(cyclohexylamino)-3-((pyridin-4-ylmethyl)amino)phenyl)sulfonamido)ethyl)piperazine-1-carboxylate **43** (0.150 g, 0.262 mmol) as starting material to afford the desired 4-(cyclohexylamino)-N-(2-(piperazin-1-yl)ethyl)-3-((pyridin-4-ylmethyl)amino)benzenesulfonamide hydrochloride **49** (0.075 g, 0.147 mmol). The reported NMR spectrum is that of the free base of **49**.

^{1}H NMR (400 MHz, DMSO-d_6) δ 1.20 - 1.54 (m, 6H), 1.66 - 1.74 (m, 1H), 1.76 - 1.86 (m, 2H), 2.01 - 2.11 (m, 2H), 2.13 - 2.26 (m, 6H), 2.57 - 2.61 (m, 2H), 2.66 (t, J = 4.7 Hz, 4H), 3.22 - 3.33 (m, 1H), 4.43 (d, J = 5.5 Hz, 2H), 5.18 (d, J = 7.2 Hz, 1H), 5.90 (t, J = 5.7 Hz, 1H), 6.62 (d, J = 8.5 Hz, 1H), 6.65 (d, J = 2.1 Hz, 1H), 6.81 (t, J = 5.5 Hz, 1H), 7.03 (dd, J = 8.3, 2.1 Hz, 1H), 7.36 - 7.44 (m, 2H), 8.54 - 8.59 (m, 2H).

^{13}C NMR (101 MHz, DMSO-d_6) δ 24.63, 25.55, 32.45, 45.41, 45.66, 50.84, 53.94, 57.31, 107.51, 107.72, 117.52, 122.26, 125.82, 134.03, 138.42, 148.82, 149.52.

t_R 1.12 min, MS (ESI) m/z 473 [M +H] (100%)

Inhibition of erastin- of ferrous ammonium sulphate-induced ferroptosis in IMR-32 neuroblastoma cells

In order to determine IC_{50}-values, human neuroblastoma cells (IMR-32) were seeded in a 96-well plate at a density of 25,000 cells/well. The next day, the cells were pretreated for 1h (in triplicates) with a $^{1}/_{3}$ dilution series of ferrostatin-1 analogues ranging from 5μM to 0.68nM and Sytox Green (1.6 μM) and a $^{1}/_{2}$ dilution series of ferrostatin-1 analogues ranging from 200 nM to 0.78nM and Sytox Green (1.6 μM) for erastin and ferrous ammonium sulphate respectively. After stimulating the cells with erastin (10μM) or ferrous ammonium sulphate (600 μM), the plate was transferred to a temperature- and CO_2-controled FLUOstar Omega fluorescence plate reader (BMG Labtech). Sytox Green intensity was measured after 13h using an excitation filter of 485 nm and an emission filter of 520 nm. In each setup, Triton-X100 (0.05%) was used to induce lyses of the cells in 6 wells/plate, and was used as 100% cell death reference. The percentage of the cell death was calculated by the formula ((AVG[erastin] - AVG[background]) / (AVG[Triton-X100] - AVG[background])) × 100. Cell death percentage was plotted in GraphPad Prism 6, and IC_{50}-values were calculated using a sigmoidal dose-response (variable slope) curve.

In vivo mouse studies

Mice were bred and housed under SPF conditions in individually ventilated cages at the VIB Inflammation Research Center in conventional, temperature-controlled animal facilities with a 14/10-hour light/dark cycle. Water and feed were provided ad libitum. Iron poisoning experiments were performed with C57BL/6N mice from Janvier Labs, toxicity of compound **39** was assessed in wild type mice derived from a Gpx4 fl/fl breeding. The present studies in animals were reviewed and approved by the Ethical committee on laboratory animal experiments of Ghent University, Faculty of Sciences, Ghent, Belgium.

Acute iron poisoning

All mice treated with iron sulfate received an intraperitoneal injection of 300 mg/kg body weight FeSO4.7H2O dissolved in sterile 0.9% NaCl or vehicle (0.9% NaCl). The injection volume was 200

μL/20 g body weight. Vehicle solution (2% DMSO) or compound was administered at a concentration of 2 mM (in 0.9% NaCl containing 2% DMSO; 200 μL / 20 g body weight) by intravenous injection 15 minutes before IP injection with FeSO4.7H2O. Two hours after iron sulfate injection, mice were anesthetized with isoflurane and blood was sampled. Hereafter, mice were sacrificed by cervical dislocation. LDH levels in plasma were measured in the clinical lab of Ghent University Hospital by COBAS 8000 (Roche).

Repeated daily injection of compound 39

Vehicle solution (2% DMSO) or compound was administered daily at a concentration of 2 mM (in 0.9% NaCl containing 2% DMSO; 200 μL / 20 g body weight) by intraperitoneal injection. Body temperature and weight were monitored daily. On day 28 the mice were anesthetized with isoflurane and blood was sampled. Hereafter, mice were sacrificed by cervical dislocation. ALT, AST and LDH levels in plasma were measured in the clinical lab of Ghent University Hospital by COBAS 8000 (Roche). CK, creatinine, urea and troponin T were determined at the lab for medical analysis CRI (https://www.cri.be/).

Bilayer insertion of UAMC-3203 occurs on the nanosecond scale

Parameters for alpha-tocopherol and UAMC3203 were generated using the Automated Topology Builder webserver after an optimization at the B3LYP/6-31G* level.[37] Charges were fitted to the elec-trostatic potential using the Merz-Singh-Kollman scheme. Water molecules were treated with the SPC water model. The system was treated using the GROMOS 54A7 force field.[38] The pre-equilibrated hydrated 128 POPC lipid box was taken from Poger and Mark.[39] A 2 fs timestep was adopted, with all bonds constrained to their equilibrium lengths using LINCS.[40] Non-bonded interactions were truncated at 1.4 nm. PME was used to account for electrostatic interactions beyond the cut-off. The system was energy-minimised with the steepest descent algorithm until the maximum force exerted on any atom was less than 1000.0 kJ/mol.nm. The system was equilibrated in the NPT ensemble for 10 ns using a semi-isotropic Berendsen[41] barostat with a reference pressure of 1 bar and a coupling time of 0.5 ps, while the

temperature was controlled through one velocity-rescaling thermostat[42] coupled to the membrane and one thermostat coupled to water and the ligand with a reference temperature of 303K and a coupling time of 0.1ps. Three separate production simulations with a length of 300 ns were per-formed following three separate 10 ns equilibrations. Pressure control was achieved through a semi-isotropic Parrinello-Rahman barostat with a coupling time of 5 ps.[43] All simulations were performed using Gromacs 2016.5.[44] The computational resources and services used in this work were provided by the VSC (Flemish Supercomputer Center), funded by the Research Foundation – Flanders (FWO) and the Flemish Government – department EWI.

AUTHOR INFORMATION

Corresponding Authors

* Koen Augustyns, Laboratory of Medicinal Chemistry (UAMC), University of Antwerp, Universiteitsplein 1, 2610 Wilrijk. Belgium, E-mail: koen.augustyns@uantwerpen.be. Phone: +3232652717.

* Tom Vanden Berghe, Molecular Signalling and Cell Death unit, VIB Center for Inflammation Research, Technologiepark 927, 9052 Zwijnaarde, Belgium, E-mail: tom.vandenberghe@irc.vib-ugent.be, Phone: +3293313721,

Author Contributions

The manuscript was written through contributions of all authors. All authors have given approval to the final version of the manuscript.

ACKNOWLEDGMENT

We would like to thank Sophie Lyssens and Ingmar Stuyver for excellent technical assistance with the determination of both the *in vitro* ADME parameters and the kinetic solubility. Also An Matheeussen's work determining the *in vivo* characteristics deserves special recognition. This research was funded by the Fonds Wetenschappelijk Onderzoek (FWO) Flanders by means of a personal grant appointed to Lars Devisscher under grant agreements no. 11Z815N and 11Z817N. This research was also financed by the FWO under grant agreements no. G078713N and G0B7118N, and by the FWO Excellence of Science program under the grant agreement no. G0G6618N (EOS ID 30826052). Sam Hofmans is paid by the University of Antwerp as a researcher to work in the Laboratory of Medicinal Chemistry. The Laboratory of Medicinal Chemistry is partner of the Antwerp Drug Discovery Network (www.addn.be). Research in the P.V. unit is supported by Belgian grants (Interuniversity Attraction Poles, IAP 7/32), Flemish grants (Research Foundation Flanders, FWO G.0875.11, FWO G.0973.11, FWO G.0A45.12, FWO G.0172.12, FWO G.0787.13N, FWO G.0C31.14N, FWO KAN 31528711, FWO KAN 1504813N and Foundation against Cancer 2012-188), Ghent University grants (MRP, GROUP-ID consortium) and grants from Flanders Institute for Biotechnology (VIB). P.V. holds a Methusalem grant (BOF09/01M00709) from the Flemish Government.

ABBREVIATIONS

TNF, Tumour Necrosis Factor; RIPK, Receptor-Interacting Protein Kinase; MLKL, Mixed-Lineage Kinase Like pseudokinase; VDAC, Voltage-Dependent Anion Channel; Fer-1, ferrostatin-1; ROS, Reactive Oxygen Species; GSH, glutathione:; GPX4, Glutathione peroxidase 4; SAR, Structure-Activity Relationship; CR, cystine reductase; GCL, glutamate cysteine lipase; γGC, γ-glutamyl cysteine; GS, glutathione synthase; GSSG, glutathione disulfide; FIN, Ferroptosis Inducer.

ANCILLIARY INFORMATION

Supporting Information. Detailed protocols, extended data series, molecular formula strings, additional charts and graphs for *in vitro* ADME analyses. This material is available free of charge via the Internet at http://pubs.acs.org.

REFERENCES

(1) Galluzzi, L.; Vitale, I.; Aaronson, S. A.; Abrams, J. M.; Adam, D.; Agostinis, P.; Alnemri, E. S.; Altucci, L.; Amelio, I.; Andrews, D. W.; Annicchiarico-Petruzzelli, M.; Antonov, A. V.; Arama, E.; Baehrecke, E. H.; Barlev, N. A.; Bazan, N. G.; Bernassola, F.; Bertrand, M. J. M.; Bianchi, K.; Blagosklonny, M. V.; Blomgren, K.; Borner, C.; Boya, P.; Brenner, C.; Campanella, M.; Candi, E.; Carmona-Gutierrez, D.; Cecconi, F.; Chan, F. K. M.; Chandel, N. S.; Cheng, E. H.; Chipuk, J. E.; Cidlowski, J. A.; Ciechanover, A.; Cohen, G. M.; Conrad, M.; Cubillos-Ruiz, J. R.; Czabotar, P. E.; D'Angiolella, V.; Dawson, T. M.; Dawson, V. L.; De Laurenzi, V.; De Maria, R.; Debatin, K. M.; Deberardinis, R. J.; Deshmukh, M.; Di Daniele, N.; Di Virgilio, F.; Dixit, V. M.; Dixon, S. J.; Duckett, C. S.; Dynlacht, B. D.; El-Deiry, W. S.; Elrod, J. W.; Fimia, G. M.; Fulda, S.; García-Sáez, A. J.; Garg, A. D.; Garrido, C.; Gavathiotis, E.; Golstein, P.; Gottlieb, E.; Green, D. R.; Greene, L. A.; Gronemeyer, H.; Gross, A.; Hajnoczky, G.; Hardwick, J. M.; Harris, I. S.; Hengartner, M. O.; Hetz, C.; Ichijo, H.; Jäättelä, M.; Joseph, B.; Jost, P. J.; Juin, P. P.; Kaiser, W. J.; Karin, M.; Kaufmann, T.; Kepp, O.; Kimchi, A.; Kitsis, R. N.; Klionsky, D. J.; Knight, R. A.; Kumar, S.; Lee, S. W.; Lemasters, J. J.; Levine, B.; Linkermann, A.; Lipton, S. A.; Lockshin, R. A.; López-Otín, C.; Lowe, S. W.; Luedde, T.; Lugli, E.; MacFarlane, M.; Madeo, F.; Malewicz, M.; Malorni, W.; Manic, G.; Marine, J. C.; Martin, S. J.; Martinou, J. C.; Medema, J. P.; Mehlen, P.; Meier, P.; Melino, S.; Miao, E. A.; Molkentin, J. D.; Moll, U. M.; Muñoz-Pinedo, C.; Nagata, S.; Nuñez, G.; Oberst, A.; Oren, M.; Overholtzer, M.; Pagano, M.; Panaretakis, T.; Pasparakis, M.; Penninger, J. M.; Pereira, D. M.; Pervaiz, S.; Peter, M. E.; Piacentini, M.; Pinton, P.; Prehn, J. H. M.; Puthalakath, H.; Rabinovich, G. A.; Rehm, M.; Rizzuto, R.; Rodrigues, C. M. P.; Rubinsztein,

D. C.; Rudel, T.; Ryan, K. M.; Sayan, E.; Scorrano, L.; Shao, F.; Shi, Y.; Silke, J.; Simon, H. U.; Sistigu, A.; Stockwell, B. R.; Strasser, A.; Szabadkai, G.; Tait, S. W. G.; Tang, D.; Tavernarakis, N.; Thorburn, A.; Tsujimoto, Y.; Turk, B.; Vanden Berghe, T.; Vandenabeele, P.; Vander Heiden, M. G.; Villunger, A.; Virgin, H. W.; Vousden, K. H.; Vucic, D.; Wagner, E. F.; Walczak, H.; Wallach, D.; Wang, Y.; Wells, J. A.; Wood, W.; Yuan, J.; Zakeri, Z.; Zhivotovsky, B.; Zitvogel, L.; Melino, G.; Kroemer, G. Molecular Mechanisms of Cell Death: Recommendations of the Nomenclature Committee on Cell Death 2018. *Cell Death Differ.* **2018**, *25* (3), 486–541.

(2) Taylor, R. C.; Cullen, S. P.; Martin, S. J. Apoptosis: Controlled Demolition at the Cellular Level. *Nat. Rev. Mol. Cell Biol.* **2008**, *9* (3), 231–241.

(3) Grootjans, S.; Vanden Berghe, T.; Vandenabeele, P. Initiation and Execution Mechanisms of Necroptosis: An Overview. *Cell Death Differ.* **2017**, *24* (7), 1184–1195.

(4) Ramirez, M. L. G.; Salvesen, G. S. A Primer on Caspase Mechanisms. *Semin. Cell Dev. Biol.* **2018**, 1–7.

(5) Vanden Berghe, T.; Linkermann, A.; Jouan-Lanhouet, S.; Walczak, H.; Vandenabeele, P. Regulated Necrosis: The Expanding Network of Non-Apoptotic Cell Death Pathways. *Nat. Rev. Mol. Cell Biol.* **2014**, *15* (2), 135–147.

(6) Conrad, M.; Angeli, J. P. F.; Vandenabeele, P.; Stockwell, B. R. Regulated Necrosis: Disease Relevance and Therapeutic Opportunities. *Nat. Rev. Drug Discov.* **2016**, 1–19.

(7) Dolma, S.; Lessnick, S. L.; Hahn, W. C.; Stockwell, B. R. Identification of Genotype-Selective Antitumor Agents Using Synthetic Lethal Chemical Screening in Engineered Human Tumor Cells. *Cancer Cell* **2003**, *3* (3), 285–296.

(8) Yagoda, N.; von Rechenberg, M.; Zaganjor, E.; Bauer, A. J.; Yang, W. S.; Fridman, D. J.; Wolpaw, A. J.; Smukste, I.; Peltier, J. M.; Boniface, J. J.; Smith, R.; Lessnick, S. L.; Sahasrabudhe,

S.; Stockwell, B. R. RAS–RAF–MEK-Dependent Oxidative Cell Death Involving Voltage-Dependent Anion Channels. *Nature* **2007**, *447* (7146), 865–869.

(9) Dixon, S. J.; Lemberg, K. M.; Lamprecht, M. R.; Skouta, R.; Zaitsev, E. M.; Gleason, C. E.; Patel, D. N.; Bauer, A. J.; Cantley, A. M.; Yang, W. S.; Morrison, B.; Stockwell, B. R. Ferroptosis: An Iron-Dependent Form of Nonapoptotic Cell Death. *Cell* **2012**, *149* (5), 1060–1072.

(10) Zilka, O.; Shah, R.; Li, B.; Friedmann Angeli, J. P.; Griesser, M.; Conrad, M.; Pratt, D. A. On the Mechanism of Cytoprotection by Ferrostatin-1 and Liproxstatin-1 and the Role of Lipid Peroxidation in Ferroptotic Cell Death. *ACS Cent. Sci.* **2017**, acscentsci.7b00028.

(11) Dixon, S. J.; Lemberg, K. M.; Lamprecht, M. R.; Skouta, R.; Zaitsev, E. M.; Gleason, C. E.; Patel, D. N.; Bauer, A. J.; Cantley, A. M.; Yang, W. S.; Morrison III, B.; Stockwell, B. R. Ferroptosis: An Iron-Dependent Form of Nonapoptotic Cell Death. *Cell* **2012**, *149* (5), 1060–1072.

(12) Cao, J. Y.; Dixon, S. J. Mechanisms of Ferroptosis. *Cell. Mol. Life Sci.* **2016**, *73* (11–12), 2195–2209.

(13) Yang, W. S.; Sriramaratnam, R.; Welsch, M. E.; Shimada, K.; Skouta, R.; Viswanathan, V. S.; Cheah, J. H.; Clemons, P. A.; Shamji, A. F.; Clish, C. B.; Brown, L. M.; Girotti, A. W.; Cornish, V. W.; Schreiber, S. L.; Stockwell, B. R. Regulation of Ferroptotic Cancer Cell Death by GPX4. *Cell* **2014**, *156* (1–2), 317–331.

(14) Seiler, A.; Schneider, M.; Förster, H.; Roth, S.; Wirth, E. K.; Culmsee, C.; Plesnila, N.; Kremmer, E.; Rådmark, O.; Wurst, W.; Bornkamm, G. W.; Schweizer, U.; Conrad, M. Glutathione Peroxidase 4 Senses and Translates Oxidative Stress into 12/15-Lipoxygenase Dependent- and AIF-Mediated Cell Death. *Cell Metab.* **2008**, *8* (3), 237–248.

(15) Brigelius-Flohé, R.; Maiorino, M. Glutathione Peroxidases. *Biochim. Biophys. Acta - Gen. Subj.* **2013**, *1830* (5), 3289–3303.

(16) Hofmans, S.; Berghe, T. Vanden; Devisscher, L.; Hassannia, B.; Lyssens, S.; Joossens, J.; Van Der Veken, P.; Vandenabeele, P.; Augustyns, K. Novel Ferroptosis Inhibitors with Improved Potency and ADME Properties. *J. Med. Chem.* **2016**, *59* (5), 2041–2053.

(17) Angeli, J. P. F.; Shah, R.; Pratt, D. A.; Conrad, M. Ferroptosis Inhibition: Mechanisms and Opportunities. *Trends Pharmacol. Sci.* **2017**, *38* (5), 489–498.

(18) Skouta, R.; Dixon, S. J.; Wang, J.; Dunn, D. E.; Orman, M.; Shimada, K.; Rosenberg, P. A.; Lo, D. C.; Weinberg, J. M.; Linkermann, A.; Stockwell, B. R. Ferrostatins Inhibit Oxidative Lipid Damage and Cell Death in Diverse Disease Models. *J Am Chem Soc* **2014**, *136* (12), 4551–4556.

(19) Friedmann Angeli, J. P.; Schneider, M.; Proneth, B.; Tyurina, Y. Y.; Tyurin, V. a; Hammond, V. J.; Herbach, N.; Aichler, M.; Walch, A.; Eggenhofer, E.; Basavarajappa, D.; Rådmark, O.; Kobayashi, S.; Seibt, T.; Beck, H.; Neff, F.; Esposito, I.; Wanke, R.; Förster, H.; Yefremova, O.; Heinrichmeyer, M.; Bornkamm, G. W.; Geissler, E. K.; Thomas, S. B.; Stockwell, B. R.; O'Donnell, V. B.; Kagan, V. E.; Schick, J. a; Conrad, M. Inactivation of the Ferroptosis Regulator Gpx4 Triggers Acute Renal Failure in Mice. *Nat. Cell Biol.* **2014**, *3* (August), 1–9.

(20) Yoo, S. E.; Chen, L.; Na, R.; Liu, Y.; Rios, C.; Van Remmen, H.; Richardson, A.; Ran, Q. Gpx4 Ablation in Adult Mice Results in a Lethal Phenotype Accompanied by Neuronal Loss in Brain. *Free Radic. Biol. Med.* **2012**, *52* (9), 1820–1827.

(21) Chen, L.; Na, R.; Gu, M.; Richardson, A.; Ran, Q. Lipid Peroxidation up-Regulates BACE1 Expression in Vivo: A Possible Early Event of Amyloidogenesis in Alzheimer's Disease. *J. Neurochem.* **2008**, *107* (1), 197–207.

(22) Sengupta, A.; Lichti, U.; Carlson, B.; Cataisson, C.; Ryscavage, A. O.; Mikulec, C.; Conrad, M.; Fischer, S. M.; Hatfield, D. L.; Yuspa, S. H. Targeted Disruption of Glutathione Peroxidase 4 in Mouse Skin Epithelial Cells Impairs Postnatal Hair Follicle Morphogenesis That Is Partially Rescued through Inhibition. *J. Invest. Dermatol.* **2013**, *133* (7), 1731–1741.

(23) Wortmann, M.; Schneider, M.; Pircher, J.; Hellfritsch, J.; Aichler, M.; Vegi, N.; Kölle, P.; Kuhlencordt, P.; Walch, A.; Pohl, U.; Bornkamm, G. W.; Conrad, M.; Beck, H. Combined Deficiency in Glutathione Peroxidase 4 and Vitamin E Causes Multiorgan Thrombus Formation and Early Death in Mice. *Circ. Res.* **2013**, *113* (4), 408–417.

(24) Ueta, T.; Inoue, T.; Furukawa, T.; Tamaki, Y.; Nakagawa, Y.; Imai, H.; Yanagi, Y. Glutathione Peroxidase 4 Is Required for Maturation of Photoreceptor Cells. *J. Biol. Chem.* **2012**, *287* (10), 7675–7682.

(25) Linkermann, A.; Skouta, R.; Himmerkus, N.; Mulay, S. R.; Dewitz, C.; De Zen, F.; Prokai, A.; Zuchtriegel, G.; Krombach, F.; Welz, P.-S.; Weinlich, R.; Vanden Berghe, T.; Vandenabeele, P.; Pasparakis, M.; Bleich, M.; Weinberg, J. M.; Reichel, C. a; Bräsen, J. H.; Kunzendorf, U.; Anders, H.-J.; Stockwell, B. R.; Green, D. R.; Krautwald, S. Synchronized Renal Tubular Cell Death Involves Ferroptosis. *Proc. Natl. Acad. Sci. U. S. A.* **2014**, *111* (47), 16836–16841.

(26) Hassannia, B.; Wiernicki, B.; Ingold, I.; Qu, F.; Van Herck, S.; Tyurina, Y. Y.; Bayır, H.; Abhari, B. A.; Angeli, J. P. F.; Choi, S. M.; Meul, E.; Heyninck, K.; Declerck, K.; Chirumamilla, C. S.; Lahtela-Kakkonen, M.; Van Camp, G.; Krysko, D. V; Ekert, P. G.; Fulda, S.; De Geest, B. G.; Conrad, M.; Kagan, V. E.; Vanden Berghe, W.; Vandenabeele, P.; Vanden Berghe, T. Nano-Targeted Induction of Dual Ferroptotic Mechanisms Eradicates High-Risk Neuroblastoma. *J. Clin. Invest.* **2018**, *128* (8), 3341–3355.

(27) Li, Q.; Han, X.; Lan, X.; Gao, Y.; Wan, J.; Durham, F.; Cheng, T.; Yang, J.; Wang, Z.; Jiang, C.; Ying, M.; Koehler, R. C.; Stockwell, B. R.; Wang, J. Inhibition of Neuronal Ferroptosis Protects Hemorrhagic Brain. *JCI Insight* **2017**, *2* (7), 1–19.

(28) Chang, L. C.; Chiang, S. K.; Chen, S. E.; Yu, Y. L.; Chou, R. H.; Chang, W. C. Heme Oxygenase-1 Mediates BAY 11–7085 Induced Ferroptosis. *Cancer Lett.* **2018**, *416*, 124–137.

(29) Gaschler, M. M.; Andia, A. A.; Liu, H.; Csuka, J. M.; Hurlocker, B.; Vaiana, C. A.; Heindel, D.

W.; Zuckerman, D. S.; Bos, P. H.; Reznik, E.; Ye, L. F.; Tyurina, Y. Y.; Lin, A. J.; Shchepinov, M. S.; Chan, A. Y.; Peguero-Pereira, E.; Fomich, M. A.; Daniels, J. D.; Bekish, A. V; Shmanai, V. V; Kagan, V. E.; Mahal, L. K.; Woerpel, K. A.; Stockwell, B. R. FINO2 Initiates Ferroptosis through GPX4 Inactivation and Iron Oxidation. *Nat. Chem. Biol.* **2018**, *14* (5), 507–515.

(30) Chang, T. P.-Y.; Rangan, C. Iron Poisoning. *Pediatr. Emerg. Care* **2011**, *27* (10), 978–985.

(31) Leung, V.; Bartfay, W. Investigations into the Systemic Production of Aldehyde-Derived Peroxidation Products in a Murine Model of Acute Iron Poisoning: A Dose Response Study . *Can. J. Physiol. Pharmacol.* **2002**, *80* (9), 851–856.

(32) Barr, J.; Berkovitch, M.; Tavori, I.; Kariv, N.; Schejter, A.; Eshel, G. Acute Iron Intoxication: The Efficacy of Deferiprone and Sodium Biocarbonate in the Prevention of Iron Absorption from the Digestive Tract. *Vet. Hum. Toxicol.* **1999**, *41* (5), 308–311.

(33) Eickholt, T. H.; White, W. F. Determination of Iron Toxicity in Mice. *J. Pharm. Sci.* **1965**, *54* (8), 1211–1213.

(34) Audimoolam, V. K.; Wendon, J.; Bernal, W.; Heaton, N.; O'Grady, J.; Auzinger, G. Iron and Acetaminophen a Fatal Combination? *Transpl. Int.* **2011**, *24* (10), 85–88.

(35) Abhilash, K. P. P.; Arul, J. J.; Bala, D. Fatal Overdose of Iron Tablets in Adults. *Indian J. Crit. Care Med.* **2013**, *17* (5), 311–313.

(36) Litwinienko, G.; Ingold, K. U. Solvent Effects on the Rates and Mechanisms of Reaction of Phenols with Free Radicals. *Acc. Chem. Res.* **2007**, *40* (3), 222–230.

(37) Koziara, K. B.; Stroet, M.; Malde, A. K.; Mark, A. E. Testing and Validation of the Automated Topology Builder (ATB) Version 2.0: Prediction of Hydration Free Enthalpies. *J. Comput. Aided. Mol. Des.* **2014**, *28* (3), 221–233.

(38) Schmid, N.; Eichenberger, A. P.; Choutko, A.; Riniker, S.; Winger, M.; Mark, A. E.; Van

Gunsteren, W. F. Definition and Testing of the GROMOS Force-Field Versions 54A7 and 54B7. *Eur. Biophys. J.* **2011**, *40* (7), 843–856.

(39) Poger, D.; Mark, A. E. On the Validation of Molecular Dynamics Simulations of Saturated and Cis -Monounsaturated Phosphatidylcholine Lipid Bilayers: A Comparison with Experiment. *J Chem Theory Comput* **2010**, *6* (1), 325–336.

(40) Hess, B.; Bekker, H.; Berendsen, H. J. C.; Fraaije, J. G. E. M. LINCS: A Linear Constraint Solver for Molecular Simulations. *J. Comput. Chem.* **1997**, *18* (12), 1463–1472.

(41) Berendsen, H. J. C.; Postma, J. P. M.; Van Gunsteren, W. F.; Dinola, A.; Haak, J. R. Molecular Dynamics with Coupling to an External Bath. *J. Chem. Phys.* **1984**, *81* (8), 3684–3690.

(42) Bussi, G.; Donadio, D.; Parrinello, M. Canonical Sampling through Velocity-Rescaling. *J. Chem. Phys.* **2008**, *126* (1).

(43) Parrinello, M.; Rahman, A. Polymorphic Transitions in Single Crystals: A New Molecular Dynamics Method. *J. Appl. Phys.* **1981**, *52* (12), 7182–7190.

(44) Abraham, M. J.; Murtola, T.; Schulz, R.; Páll, S.; Smith, J. C.; Hess, B.; Lindah, E. Gromacs: High Performance Molecular Simulations through Multi-Level Parallelism from Laptops to Supercomputers. *SoftwareX* **2015**, *1–2*, 19–25.

TABLE OF CONTENTS GRAPHIC

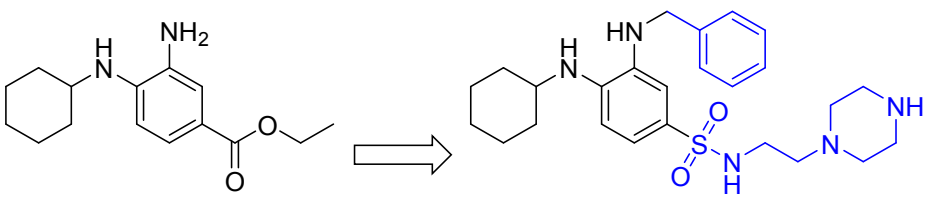

1
(Fer-1)

Ferroptosis IC_{50} = 33 nM

39
(UAMC-3203)

Ferroptosis IC_{50} = 12 nM

Microsomal stability
$t_{1/2}$(Human) = 20.5 h
$t_{1/2}$(Rat) = 16.5 h
$t_{1/2}$(Mouse) = 3.5 h

Plasma recovery after 6h
%(Human) = 84.2
%(Rat) = 85.8
%(Mouse) = 100